MATHEMATICAL MODEL STUDIES OF FLOW FIELDS IN COMBINATION BLOWN STEELMAKING SYSTEMS

A Thesis Submitted
in Partial Fulfilment of the Requirements
for the Degree of

MASTER OF TECHNOLOGY

by

DEVULAPALLI BALAJI

to the

DEPARTMENT OF METALLURGICAL ENGINEERING
INDIAN INSTITUTE OF TECHNOLOGY KANPUR
FEBRUARY, 1990

CERTIFICATE

This is to certify that the present work 'MATHEMATICAL MODEL STUDIES OF FLOW FIELDS IN COMBINATION BLOWN STEELMAKING SYSTEMS', has been carried out by Mr. D. Balaji under my supervision and that this has not been submitted elsewhere for a degree.

February 1990

Dipak Mazumdar

(Dr. Dipak Mazumdar)
Assistant Professor
Department of Metallurgical Engineering
Indian Institute of Technology
Kanpur

ACKNOWLEDGENT

I am deeply indebted to Dr. Dipak Mazumdar , my mentor, for his valuable guidence, support, brilliant ideas and inspiration without which it would not have been possible to complete this work.

I would like to thank Mr. V. P. Gupta for his excellent drawings before the deadline of the submission.

A special note of thanks to Manju, K. P. Singh(Ravi), Venkat, Tripp, Mamashri(Prasad), Gopi. K, Deepu, Hanu, Nagu and many others for making my stay at I. I. T. Kanpur most memorable.

Finally, I could not find words to express my feelings towards my parents for their moral support and constant encouragement throughout my life.

I. I. T Kanpur

Balaji Devulapalli

TABLE OF CONTENTS

ABSTRACT

Hydrodynamics of an axi-symmetric combination blown steelmaking process has been analysed mathematically. The recirculatory flow field within the reactor vessel has been represented interms of the turbulent Navier-Stokes equations in conjunction with the $k-\varepsilon$ turbulence model and the resultant set of partial differential equations together with the appropriate boundary conditions solved via a control volume based finite difference procedure embodied in the popular TEACH-T computer code. Prior to any evaluation of the model predictions, sensitivity of computations to the choice of residual value, noda configurations and differencing schemes (e.g., upwind, hybrid, exponential, power law etc.) have been assessed and results independent of these established.

The bottom/submerged gas injection phenomena in a combined blowing reactor has been represented via the single phase variable density formulation technique, wherein the rising two phase gas-liquid mixture has been treated like a homogeneous fluid of reduced density. The gas volume fraction and hence the density of the two phase mixture have been estimated from a knowledge of the dimensions of the two phase region and the latter's average rise velocity. To this end, several calculation procedures (viz., formulations based on slip vs no-slip, constant gas volume fraction vs variable gas volume fraction in the gas-liquid plume etc.) reported in the literature have been critically examined. Through extensive comparisons between theory and experiments it is demonstrated that the bottom injection phenomena can be mathematically adequately represented by assuming gas/bubble

slippage and considering a constant rise velocity of the two phase mixture.

In representing the impinging gas jet (e.g.,the top gas injection system) the shearing force imparted by the outwardly flowing gas across the cavity surface (e.g.,the gas-liquid interface) has so far been assumed to be the only mechanism producing the bulk liquid recirculation. However, the present investigation appears to suggest that flows generated through such considerations alone are not sufficient enough to drive the flow recirculation observed experimentally. Consequently, as an additional mechanism to the shearing force, the force of impingement estimated from the increased potential energy of the melt (viz., deduced from the corresponding increase in bath height) has been considered and the top blowing system represented accordingly via an approach based on these two mechanisms. Flow fields thus predicted have been evaluated against equivalent experimental measurements on water models and excellent agreement achieved. Finally, hydrodynamic models of top and bottom injection systems have been coupled and a steady state fluid flow model for combination blown steelmaking system proposed. Numerical predictions from the model have also been evaluated against experimental measurements and reasonably good agreement between theory and experiments demonstrated.

NOMENCLATURE

A_P, A_N, A_E, A_W, A_S	Coefficients of discretization equation representing the effect of convection and diffusion
A_{nb}	Summation of all neighbour point coefficients
C_a	Constant defined in (I.4): has a value of 7
C_D	Dissipation rate constant : has a value of 0.09
C_g	Constant defined in (I.5): has a value of 0.12
C_r	Constant defined in (I.4): has a value of 0.107
C_t	Constant defined in (I.6): has a value of 9.1
C_1	Constant defined in (II.10): has a value of 1.43
C_2	Constant defined in (II.10): has a value of 1.92
d	Diameter of a lance nozzle, m
d_B	Diameter of a gas bubble, m
g	Acceleration due to gravity, m s^{-2}
H	Height of the liquid bath, m
h_O	Distance between analytic origin and the base of the vessel, m

K	Constant defined in (I.4): has a value of 1.0
k	Turbulence kinetic energy, $m^2 s^{-2}$
l_o	Distance between orifice of lance nozzle and free surface, m
p	Pressure within the liquid, Pa
Q_g, Q	Gas flow rate, m^3/s
r	the radial coordinate, m
R	Radius of the bath, m
r_c	Radius of the two phase plume, m
R_L	Sum of residual source
U_p	Constant plume velocity, m/s
U_s	Bubble slip velocity, m/s
J_z	Mixture rise velocity in the two phase region, m/s
u	Axial velocity component, m/s
v	Radial velocity component, m/s
v_b	Volume fraction of the bulk phase in a control volume
f	Volume fraction of the two phase region in control volume
	the axial coordinate, m
	Gas void fraction
n	Gas void fraction at the axis of symmetry
	Shear stress acting across the cavity surface, kg $m^{-1} s^{-2}$

ρ_g	Density of gas, kg m^{-3}
ρ_L	Density of liquid, kg m^{-3}
μ_g	Viscosity of the gas, kg $m^{-1}s^{-1}$
μ_{eff}	Effective viscosity, kg $m^{-1}s^{-1}$
μ_T	Turbulence viscosity, kg $m^{-1}s^{-1}$
μ_L	Laminar viscosity, kg $m^{-1}s^{-1}$
ε	Turbulence kinetic energy dissipation rate per unit mass, m^2s^{-3}
σ_k	Constant in the $k-\varepsilon$ model : has a value of 1.0
σ_ε	Constant in the $k-\varepsilon$ model : has a value of 1.3
$\emptyset$	Any general variable
λ	Half jet cone angle, radians

List Of Figures

List Of Tables

CHAPTER I

INTRODUCTION

I.1 Introduction To The Thesis

The injection of reactive and non-reactive gases into melts contained in metallurgical furnaces, ladles etc. is a frequent phenomena encountered in numerous metal processing operations. In either case,the injected gas promotes fluid motion within the vessel and thereby exerts considerable influences on phenomena, such as, slag-metal reactions,thermal and particulate homogenisation, inclusion float out or re-entrainment etc.. Consequently, gas injection induced stirring in metallurgical reactors has since long been the subject of considerable interest. Moreover,this has been recognized to be of vital importance in determining the efficiency of numerous associated processes (viz.,melting/dissolution, dispersion/mixing etc.) carried out in gas stirred reactors.

Typically, two different modes of gas injection have been applied to produce the required stirring and these include :

(i) gas jet impinging on the surface of metallic melts

and

(ii)subsurface injection of gas through a lance, tuyere or porous-plug.

As an example to the first category,mention can be made of the top blown oxygen steelmaking system(viz.,the LD process) while for the latter, depending on the intensity of the blow a wide range of metal processing operations (viz., from bottom blown steelmaking processes to ladle processing of steel) may be cited. It has been realised for some time that the intensity of

bath stirring in top blown reactors is relatively sluggish, as the transfer of momentum from the impinging gas stream to the bulk liquid phase is rather inefficient. On the contrary,bottom injection provides vigorous bath agitation and thus exacerbates the rates of various mass transfer controlled phenomena, characteristic of high temperature operations. Indeed, in combination blown steelmaking processes desired metallurgical results have been successfully obtained by judiciously combining the top (this supplies the necessary oxygen for metalloid oxidation reactions) and the bottom/submerged gas injection systems (see Fig. I.1). Since the primary objective of the bottom gas injection system in a combined blown reactor is to provide necessary stirring rather than supply oxygen (the latter is known to be detrimental, since the bottom/tuyere life decreases by injecting oxygen through the bottom, affecting considerably the turnover rates per converter), consequently injection of inert gases like argon etc. have been typically practised. Furthermore, the "gas-liquid coupling" in submerged gas injection being more efficient (than an impinging gas jet system), requires a small volume of gas to be injected in relation to the top blown gas volume (typically about 5%) to produce the required stirring effect.

Since the flow fields induced in combined blown reactors (say, the Q-BOP) play paramount roles in controlling the associated processes, such as slag-metal reaction rates, melting/dissolution of scrap, refractory lining wear etc. consequently, adequate knowledge of bath hydrodynamics is critical to the overall process analysis. However, since high temperature, visual opacity and relatively large sizes of metallurgical

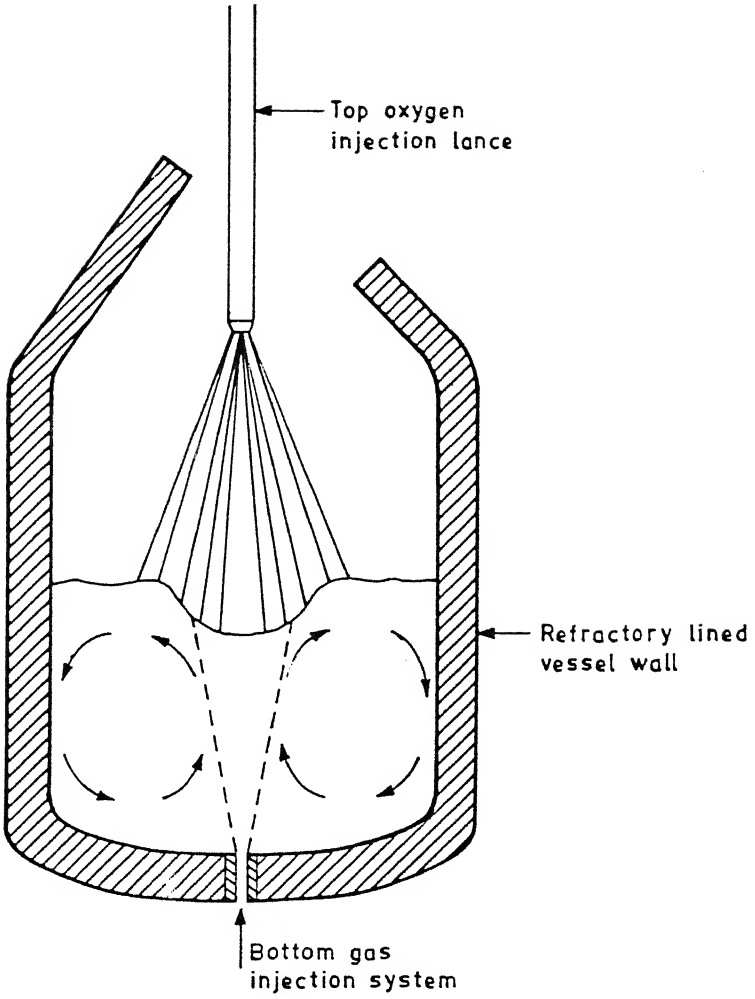

Fig. I.1. The combination blowing steel making system.

reactors pose serious limitations to direct experimental observations, consequently, an alternative approach such as cold model studies/mathematical modelling (or both in conjunction) has to be adopted to develop understanding of fluid flow and other associated phenomena.

In the present work, hydrodynamics of a combination blown steelmaking process has been modelled mathematically and the model predictions assessed against experimental work reported in the literature on equivalent room temperature physical models (e.g.,water models). Towards these, at the onset, a brief review of relevant literature has been presented and the scope of the present work discussed. In subsequent chapters, the development of the mathematical model and the numerical modelling techniques have been outlined in detail and finally, several computed results have been compared against experimental observations. Summary and conclusions as well as recommendations for further work appear respectively in the concluding chapters. Computer programs etc. have also been assembled in an Appendix.

I.2 Review Of Relevant Literature

During the last two decades or so numerous investigations have been carried out on the combination blown steelmaking process and phenomena such as, mixing, slag-metal reactions, mass transfer rates etc. have been extensively studied. However, fluid flow aspects of the combination blown process has remained relatively less well investigated. Furthermore, little or no effort has so far been made to address fluid dynamics of such systems from mathematical points of view. Consequently, barring only one instance, no studies on mathematical modelling of combination blown process have been reported in the literature. Similarly, mathematical model studies of the top gas injection system (viz., the LD configuration) has also been rare and only one such study so far have been noted. In contrast, however, a large number of investigations on the mathematical modelling of submerged gas injection systems appear in the literature. Since combination blown process embodies both top and bottom injection systems, consequently, fluid model studies on these systems have also been included in the present review in addition to those on combination blown system.

The bottom/submerged gas injection system in the combined blowing reactor involves the injection of gas into the melt through one or a number of tuyeres located at the base of the vessel. Since the volume of gas injected through the bottom is typically small, the injection process consequently, leads to phenomena similar to those observed in ladle processing of steel. The injected gas in the immediate vicinity of the tuyeres rapidly

devolves into plumes of spherical cap bubbles, rise due to buoyancy, imparting energy to the bulk liquid and leaves the vessel through the free surface. Therefore, it is more appropriate to consider a buoyant plume rather than a jet model to describe the bottom injection phenomena. The interactions between the gas and the surrounding liquid induces flow recirculation in the vessel as has been mentioned already and this facilitates many metallurgical processes, such as, slag-metal reactions, dissolution, mixing etc..

There are two different computational procedures typically been adopted to mathematically describe the hydrodynamics of such two phase buoyancy driven systems and these include:

(a) models derived on basis of Eulerian frame of reference, which are further classified into two groups viz.,

(i) the two phase models

(ii) the quasi-single phase models

and

(b) models derived on the basis of Lagrangian frame of reference.

In the two phase modelling, two sets of continuity and momentum equations are solved, one for each phase[1]. This approach of modelling being relatively more complex from the computational view points, has therefore, received less attention in the literature. Momentum equations for individual phases are interlinked via the interface friction factor(e.g.,slip) and in addition, no assumption is made about the gas volume fraction (viz.,voidage) distribution in the plume. The latter is

rather estimated through the solution of the gas phase continuity and momentum equations.

The quasi-single phase modelling involves solution of only one set of continuity and momentum equations. Such an approach, however, requires a prior specification (either estimated or empirical)of the plume geometry (viz.,the gas- liquid zone) as well as the gas voidage. The buoyancy force per unit volume ($\rho_L g\alpha$) estimated on the basis of the assigned gas voidage (viz.,α) is added to the vertical direction momentum equation as the required driving force. Eulerian single phase modelling has received considerable attention in the literature because of its relative simplicity and ease of computational efforts. This technique, for example, has been used extensively by Debroy et al.[2], Szekely and coworkers[3,4], Sahai and Guthrie[5,6] and Mazumdar and Guthrie[7,8] to describe turbulent recirculatory flow fields in bubble stirred ladles.

In the latter approach,(e.g.,(b)) the second phase(i.e.,the gas) is treated essentially by a Lagrangian technique, in which a bubble trajectory equation is used in addition to the liquid phase continuity and momentum equations(the latter are same as those in the quasi- single phase modelling). The bubble trajectory equation together with the momentum equations provide estimates of the two phase region, gas voidage etc.[9].

Of the three approaches of modelling a submerged gas injection system mentioned above, the quasi-single phase modelling technique has been more popular. Consequently, the present literature review on the mathematical modelling of the

bottom/submerged gas injection system has been restricted to the studies based on such an approach only.

Debroy, Majumdar and Spalding[2] were the first to introduce the concept of a buoyancy driven plume in the metallurgical ladles. They considered the density deficit between the gas and the liquid phases to be the driving force (viz., the buoyancy) producing the flow recirculation and modelled this effect through adding the buoyancy force term to the axial direction momentum equation. The authors[2] adopted the Eulerian single phase modelling approach (i.e., one set of continuity and momentum equations) together with a bulk effective viscosity model[10] for describing the turbulent flow in the system. Symmetry conditions were applied to all the variables (since the configuration considered was axi-symmetric). In order to estimate the density deficit (or the void fraction) in the two phase region, zero slip condition (i.e., the gas and the liquid move together) has been applied. Numerical predictions of flow variables were assessed against experimental measurements of Szekely et al.[11] and qualitative agreement between theory and experiments have been demonstrated.

El-kaddah and Szekely[3] proposed a fluid flow based mathematical model for estimating sulphur partitioning between slag and the metal phases in a gas stirred ladle. The desulphurisation kinetics was described through prediction of turbulent flow fields via the solution of Navier-Stokes equation in conjunction with the k-ε[12] model. The calculation procedure in addition involved prior specification of gas voidage(α) through the solution of an ordinary differential equation, viz.,

$$\frac{dU_z}{dz} + \frac{U_z}{z} = \frac{\pi Q_g g}{[2 (\tan\lambda)^2 u_z^2 z^2]} \quad \ldots(I.1)$$

and incorporating in an expression, viz.,

$$\alpha(z) = \frac{[Q_g - \pi r_c^2 \alpha(1-\alpha) U_s]}{2\pi \int_0^{r_c} r U_z \, dr} \quad \ldots(I.2)$$

in which U_s is the slip velocity. Fluid flow based predictions were compared with the observed rate of desulphurisation deduced from high temperature melts and reasonably good agreement between theoretical and experimental results has been reported.

Grevet, Szekely and El-Kaddah[4] subsequently reported an extensive fluid flow study in a water model of an argon stirred ladle. In this investigation, Eulerian single phase modelling together with an assumption of bubble slippage have been incorporated. The formulation of governing equations etc. were essentially identical to those reported earlier by El-Kaddah and Szekely[3]. Excellent agreement between predicted and experimental velocity fields (deduced through Laser Doppler Velocimeter) was achieved. However, predicted and experimental turbulence kinetic energy were only in moderate agreement. The authors[4] acknowledged that such discrepancies were perhaps associated with the incorrect selection of constants or with the inherent shortcomings of the k-ε turbulence model for representing such recirculatory flow systems. Furthermore, the authors[4] suggested

that the principal mechanism of momentum transfer in bubble driven systems is due to fluid convection, (rather than turbulent diffusion) and thus predictions regarding the velocity fields were not expected to be very sensitive to the choice of a turbulence model.

Sahai and Guthrie[5,6] through their extensive experimental and theoretical studies, postulated that bubbles forming at nozzles or orifices rapidly devolve into a plume of spherical cap bubbles and that this is true for many gas injection processes carried out in holding or transfer vessels. The rising bubbles impart energy to the surrounding liquid and produce flow recirculation within the vessel. Equating the total energy supplied by the bubbles to the turbulence energy dissipation losses in the bath, a simple macroscopic expression for estimating the average rise velocity of the bubble plume has been proposed according to :

$$U_p = 4.4 \left(\frac{Q^{1/3} L^{1/4}}{R^{1/3}} \right) \quad \ldots (I.3)$$

In subsequent numerical prediction of flow etc., they adopted the above relationship to estimate the gas voidage (they considered no slip condition) in the two phase region. Furthermore, fixed velocity at the axis of the vessel has been applied as the required boundary condition instead of the typical zero gradient conditions. Predicted values were compared with experimental measurements of their own as well as with those of Lehner et al.[13] and reasonable agreement between theory and experiments has been demonstrated.

Mazumdar and Guthrie[7,8] proposed hydrodynamic models for various axisymmetric gas injection configurations found in the industrial ladle refining operations. The authors estimated gas void fraction via equation (I.3). The hydrodynamic model in essence was based on the solution of turbulent Navier-Stokes equation together with the k-ε turbulence model. Due to some discrepancy between theory and predictions for the CAS configuration[4] the empirical constants in the k-ε model were changed by some adhoc values. Numerically predicted values (flow and turbulence parameters) thus obtained were shown to be in excellent agreement with experimental results.

Salcudean and coworkers[14] proposed a three dimensional calculation procedure to describe non-axisymmetric gas injection configurations through the solution of turbulent Navier-Stokes equation, incorporating the k-ε turbulence model. There were, however, large discrepancies between theoretical estimates and experimental measurements particularly in the immediate vicinity of the nozzle. Even though good agreement between predicted and experimental values were shown for elsewhere, the authors suggested that the discrepancy could be from numerical errors due to false diffusion phenomena (e.g., related to the use of the differencing scheme etc.) as well as due to the empirical constants employed in the k-ε turbelence model.

In contrast to these, not much information is available in the literature on the mathematical modelling of top injection system. However, some studies[15,16] report advantages of bottom injection over top injection processes but donot address these from fundamental/mathematical point of view. Asai and Szekely[17] were first to propose a mathematical model for the top injection systems. The authors formulated the flow problem by the stream function-vorticity based method[18] together with the Prandtl-Kolmogorov[19] formula to calculate the turbulent viscosity. Numerically predicted results[17] gave qualitative but not quantitative agreement with experimental measurements reported earlier by Wakelin[20] on the CO_2-water systems. Even though the authors reported reasonable agreement between numerical predictions and experimental measurements, the assumptions incorporated in the model were paid very little or no attention (viz., the shape of the cavity was assumed to be known and the vorticity considered spatially uniform, an adjustable parameter over the cavity surface etc.). Furthermore, the mechanism leading to the transfer of momentum from the jet to the liquid bath was also not adequately considered and properly justified.

Zhang et al.[21] proposed a mathematical model for combined top and bottom blowing steelmaking process. The problem was formulated by statements of the turbulent transport equations for stream function and vorticity incorporating the k-ε model. To describe the top injection process, the authors considered the momentum transfer from the impinging gas jet to the bulk liquid via shear stresses acting over the cavity surface (Fig. I.1). They[21] further related the momentum flux (i.e., shear stress)

across the cavity surface to the velocity gradient and the viscosity of the gas (see also later) by an empirical relation :

$$\tau(r) = \frac{4\, C_a\, Q_g\, \mu_g}{K\, \pi^{1/2}\, l_0\, d^2} \exp\left[-\left(\frac{r}{3\, C_r\, l_0}\right)^2\right] \qquad \ldots(I.4)$$

In which C_a, K and C_r are the empirical constants (for other symbols, refer to the nomenclature).

The associated bottom injection phenomena was modelled by the quasi-single phase modelling approach. However, the plume geometry was not assumed to be known (rather estimated) and gas void fraction accordingly was deduced from a new empirical relation:

$$\alpha(r,z) = \alpha_m \exp\left[-\frac{r^2}{C_g^2 (H-Z+h_0)^2}\right] \qquad \ldots.(I.5)$$

where α_m is the void fraction at the axis of symmetry and is given as:

$$\alpha_m(z) = C_t\, Q_g^{2/3} \left[\frac{\rho_L}{(\rho_L-\rho_g)g}\right]^{1/3} (H-Z+h_0)^{-3/5} \qquad \ldots(I.6)$$

Numerically predicted flow patterns were compared with experimental measurements and qualitative agreement between the two has been demonstrated.

I.3 Scope Of The Present Work

The brief literature review presented in section I.2 clearly indicates that hydrodynamic modelling of combined top and bottom blowing steelmaking processes has practically received little or no attention. Since fluid dynamics play key roles in determining the overall process efficiency and that adequate informations on flow variables etc. in high temperature metallurgical reactors can be usefully derived via mathematical model studies, it is therefore, appropriate to direct some efforts in this direction so that some understanding of the hydrodynamics of a combination blown steel making process can be developed and used to draw useful inferences on associated phenomena such as, scrap dissolution, refractory wear, slag-metal reactions etc..

So far, as has been pointed out already, a mathematical model describing the turbulent recirculatory flow in a combined blown reactor vessel has been proposed by Zhang and coworkers[21]. The model predictions, however, have not been rigorously evaluated against equivalent experimental measurements. Experimental flow patterns have only been assessed against theoretical predictions and qualitative agreement between the two has been claimed. Since detailed flow measurement studies carried out on aqueous models of similar systems have been reported subsequently by investigators elsewhere, consequently the procedure adopted (as well the assumptions incorporated in the mathematical model)[21] by Zhang et al. needs to be re-evaluated. Furthermore, Zhang and coworkers have also employed a new calculation procedure to model the bottom injection system that is much different from the procedures

adopted by the previous investigators[2-8]. Since numerous calculation procedures can be applied to represent the bottom/submerged gas injection system, consequently, the procedure adopted by Zhang et al.as well as the suggested superiorty of their technique above those of others require critical examination. This follows since no rigorous comparison between theory and experiments have been made to justify the assertions made[21].

Finally, the investigation of Zhang and coworkers appears to suggest that the transfer of momentum from the impinging gas phase to the bulk liquid takes place only via the shear stress acting across the cavity surface. Consequently, the shearing force has been considered to be the only likely mechanism driving the flow field and accordingly, a hydrodynamic model based on this concept has been proposed[21]. However, no evidence has been put forward to justify such considerations. In view of the fact that numerous metallurgical systems are driven by potential energy (viz., filling ladles, bubble stirred ladles etc.), the assumption of a " shear force driven flow " clearly warrants some additional considerations. It is with all these preceeding objectives in mind that the present research program has been initiated. To these ends relevant details have been summarised in the subsequent sections.

CHAPTER II

THEORETICAL CONSIDERATIONS

II.1 Assumptions In Modelling

Combined top and bottom injection of gas into melts contained in industrial steelmaking units involve numerous processes that are inherently multidimensional in nature. The interactions among the various phases (viz., slag,metal and gas) present in the reactor vessel invariably lead to numerous complex phenomena, which include for example, waves and droplet formation at the free surface, thermal and particulate gradients in the melt, slag entrainment and so on. Consequently, to describe the gas injection induced flow in such multiphase and multidimensional systems via an appropriate mathematical frame work, several idealisations have to be made and accordingly, numerous assumptions need to be invoked.

In the present work, the fluid-flow model for the combination blown process has been derived incorporating the following assumptions,e.g.,

(i) gas injection into a cylindrical vessel has been considered and the presence of upper slag phases in the system has been ignored,

(ii) the wavy free surface at the top has been considered to be essentially flat,

(iii) the gas is injected through a nozzle located at the base of the vessel as well as a lance placed above the melt. The effect of multiple nozzles and tuyeres have therefore, been neglected. Furthermore, the top as well as bottom gas injection systems within the cylindrical reactor have been considered to be placed along the

symmetry axis. Consequently, cylindrical symmetry of the system has been assumed and hence, variation of the flow properties along the θ direction has been ignored,

(iv) the bubble plume formed as a result of the submerged gas injection has been idealised and its geometry and dimensions have been assumed to be known,

(v) the shape of the cavity at the free surface resulting from the impinging gas jet has been assumed to be parabolic and the dimensions of the latter known,

(vi) the recirculating flow in the reactor has been considered to be driven by the shearing forces imposed by the impinging gas jet and the buoyancy force exerted by the rising bubbles from the submerged gas injection system,

(vii) the system is essentially isothermal

and finally,

(viii) the induced flow is turbulent in nature.

A schematic of the idealised system used for the present mathematical model representation is shown in Fig II.1.

II.2 The Governing Equations

Under the imposed assumption of cylindrical symmetry, the flow variables have been assumed to be invariant along the θ co-ordinate and hence interms of the cylindrical polar co-ordinate system (r,θ and z), the statement of the problem may be conveniently formulated via a two dimensional elliptic (e.g.,the flow is recirculating) turbulent flow model[2-8] (viz.,a set of flow equations in conjunction with an appropriate turbulence model).

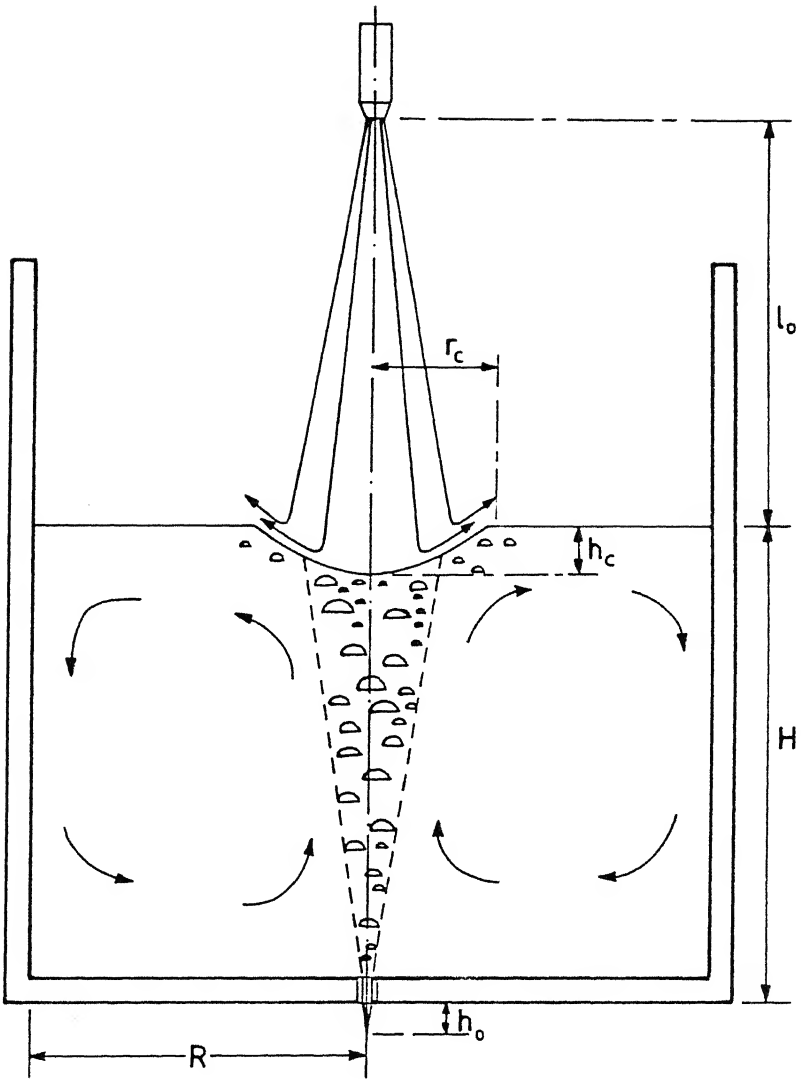

Fig. II.1. Schematic diagram of the idealised combination blown system used for the present mathematical representation.

II.2.a The flow equations

The flow equations in essence are the turbulent Navier-Stokes equations (viz.,an equation of continuity with two seperate equations for z (the axial) and r (the radial) directional momentum/motion) and are represented below :

Equation of continuity

$$\frac{\partial u}{\partial z} + \frac{1}{r}\frac{\partial (rv)}{\partial r} = 0 \qquad \ldots\ldots(II.1)$$

Equation of motion in axial direction

$$\frac{\partial}{\partial z}(\rho uu) + \frac{1}{r}\frac{\partial}{\partial r}(\rho ruv) = -\frac{\partial p}{\partial z} + \frac{\partial}{\partial z}\left(\mu_{eff}\frac{\partial u}{\partial z}\right) + \frac{1}{r}\frac{\partial}{\partial r}\left(r\mu_{eff}\frac{\partial u}{\partial r}\right) + S_u$$

$$\ldots\ldots(II.2)$$

where,

$$S_u = \frac{\partial}{\partial z}\left(\mu_{eff}\frac{\partial u}{\partial z}\right) + \frac{1}{r}\frac{\partial}{\partial r}\left(r\mu_{eff}\frac{\partial v}{\partial z}\right) + F_B + F_{s,z} \qquad \ldots\ldots(II.3)$$

Equation of motion in radial direction

$$\frac{\partial}{\partial z}(\rho uv) + \frac{1}{r}\frac{\partial}{\partial r}(\rho rvv) = -\frac{\partial p}{\partial r} + \frac{\partial}{\partial z}\left(\mu_{eff}\frac{\partial v}{\partial z}\right) + \frac{1}{r}\frac{\partial}{\partial r}\left(r\mu_{eff}\frac{\partial v}{\partial r}\right) + S_v$$

$$\ldots\ldots(II.4)$$

where,

$$S_v = \frac{\partial}{\partial z}\left(\mu_{eff}\frac{\partial u}{\partial r}\right) + \frac{1}{r}\frac{\partial}{\partial r}\left(r\mu_{eff}\frac{\partial v}{\partial r}\right) - \mu_{eff}\frac{v}{r^2} + F_{s,r} \quad \ldots\ldots(II.5)$$

F_s's and F_B in equations (II.3) and (II.5) are respectively the shear force and the buoyancy force per unit volume imposed by the top and bottom gas injection systems and are essentially the driving forces producing the flow recirculation in the combination blown reactor. These will be quantified interms of appropriate expressions in the subsequent sections.

II.2.2 The turbulence model

The effective viscosity ($\mu_{eff} \cong \mu_T$), appearing in equations (II.2) through (II.5) follows from a turbulence model and in the present investigation, the popular and the most widely used[3-8] turbulence model of Launder and Spalding[12] (viz.,the k-ε model) has been adopted. The governing transport equations for the turbulence kinetic energy, k, and its dissipation rate, ε, can be represented interms of the cylindrical polar coordinates as:

Equation of turbulence kinetic energy

$$\frac{\partial}{\partial z}(\rho u k) + \frac{1}{r}\frac{\partial}{\partial r}(\rho r v k) = \frac{\partial}{\partial z}\left(\frac{\mu_{eff}}{\sigma_k}\frac{\partial k}{\partial z}\right) + \frac{1}{r}\frac{\partial}{\partial r}\left(r\frac{\mu_{eff}}{\sigma_k}\frac{\partial k}{\partial r}\right) + S_k$$

$\ldots\ldots(II.6)$

in which, S_k, the net source term can be represented as

$$S_k = G - \rho\varepsilon \quad \text{.....(II.7)}$$

where,

$$G = \mu_T \{ 2 [(\frac{\partial u}{\partial z})^2 + (\frac{\partial v}{\partial r})^2 + (\frac{v}{r})^2] + (\frac{\partial u}{\partial r} + \frac{\partial v}{\partial z})^2 \} \quad \text{.....(II.8)}$$

Equation of dissipation rate of turbulence kinetic energy

$$\frac{\partial}{\partial r}(\rho u \varepsilon) + \frac{1}{r}\frac{\partial}{\partial r}(\rho r v \varepsilon) = \frac{\partial}{\partial z}(\frac{\mu_{eff}}{\sigma_\varepsilon}\frac{\partial \varepsilon}{\partial z}) + \frac{1}{r}\frac{\partial}{\partial r}(r\frac{\mu_{eff}}{\sigma_\varepsilon}\frac{\partial \varepsilon}{\partial r}) + S_\varepsilon \quad \text{.. (II.9}$$

where

$$S_\varepsilon = \frac{C_1 \varepsilon G}{k} + \frac{C_2 \rho \varepsilon^2}{k} \quad \text{...(II.10)}$$

The auxilary relationships embodied in the above set of equations (viz., equations(II.2) to (II.9)) are :

$$\mu_{eff} = \mu_L + \mu_T \quad \text{.....(II.11)}$$

$$\mu_T = C_D \rho k^2 / \varepsilon \quad \text{.....(II.12)}$$

and finally,

$$\rho = \alpha \rho_G + (1-\alpha) \rho_L \quad \text{....(II.13)}$$

The gas volume fraction, α, appearing in equation (II.13) is finite and non-zero only within the plume region (i.e., $0 < r < r_c$). Elsewhere in

the domain, ($r > r_c$), α is zero and consequently, $\rho=\rho_L$. The five empirical constants (viz.,C_1, C_2, C_μ, σ_ε and σ_k) embodied in the k-ε turbulence model were assigned the values according to the recommendations of Launder and Spalding. These are summarised in Table II.1.

II.3 Modelling Of The Bottom/Submerged gas Injection Process

As mentioned in the preceeding sections, the bottom injection system in the combined blown reactor has been mathematically modelled via the quasi-single phase approach (viz.,the variable density formulation) assuming that the dimensions of the rising two phase region (viz.,the bubble plume) is known (typically an empirically determined parameter). The buoyancy force exerted by the rising bubbles within the two phase region acts vertically upwards (viz.,along the axial direction) and consequently, F_B, the buoyancy force per unit volume($=\rho_L g\alpha$)$^{(2-8)}$ has been added to the axial direction momentum equation (see equation (II.3)).It is instructive to note here that α, gas volume fraction is finite and non-zero only within the two phase region. It is through the prior presciption of the gas volume fraction,α, within the two phase region that the buoyancy force resulting from the submerged gas injection system has been modelled in the present work.

The gas volume fraction within the plume can be estimated readily applying the principle of volume continuity and towards this, numerous alternative approaches exist (see also latter). Typically, the rise velocity of the gas-liquid mixture is estimated first and then from the knowledge of the plume dimensions, the gas volume fraction,α, is conveniently deduced via either,

Table II.1 Values of Constants in the k-ε Turbulence Model

C_1	C_2	σ_k	σ_ε	C_D
1.43	1.92	1.00	1.30	0.09

$$\alpha(z) = \frac{Q_g}{2\pi \int_0^{r_c} U_z r \, dr} \quad \ldots.(II.14)$$

if zero slip is assumed, or,

$$\alpha(z) = \frac{Q_g - \pi r_c^2 \alpha(1-\alpha) U_s}{2\pi \int_0^{r_c} U_z r \, dr} \quad \ldots.(II.15)$$

if slip conditions are applied.

In equations (II.14) and (II.15), r_c represents the radius of the two phase plume and U_z the rise velocity of the gas-liquid mixture at any axial station, z. Further, U_s in equation (II.15), is the slip velocity and is conventionally deduced from the knowledge of average bubble sizes in the system.

The density field distribution (viz., ρ in equations (II.2), (II.3) etc.) in the flow domain has been derived on the basis of the continum approach (viz.,equation (II.13)) and the density field established *a priori*. This is illustrated Fig II.2.

II.4 Modelling Of The Top Gas Injection System

The configuration of the impinging gas system together with the resultant cavity formed on the melt free surface have already been illustrated schematically in Fig I.1 and Fig. II.1 respectively. To mathematically model the flow induced by such top gas injection system, Asai and Szekely[17] as well as Zhang and coworkers[21] assumed that the geometry as well as the physical dimension of the cavity are known and further considered that shear stresses

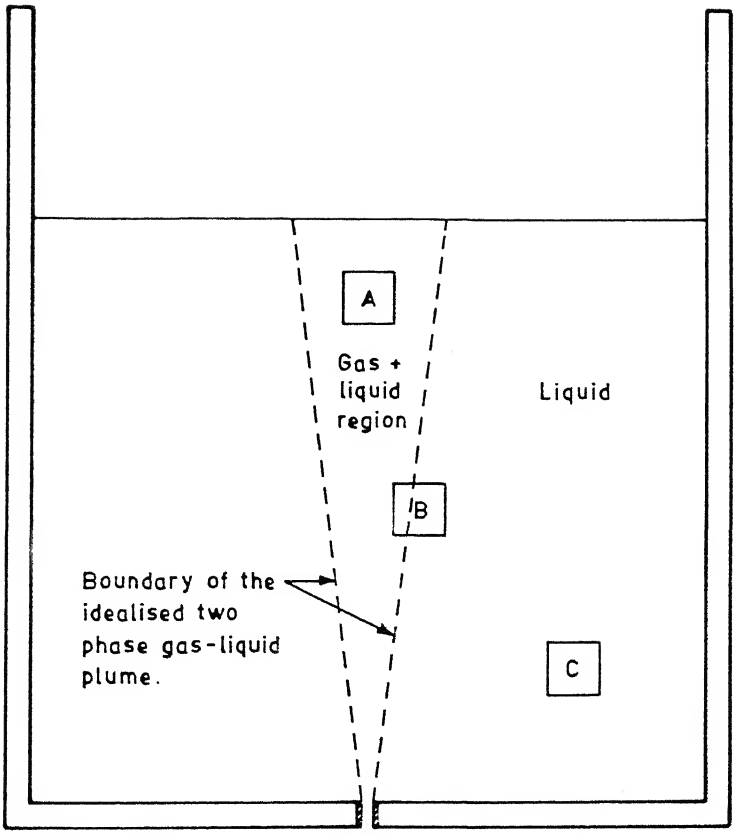

Three types of control volumes

Control volume A (completely inside the two phase plume)

$$\rho \simeq (1-\alpha)\rho_L$$

Control volume B (partly inside the two phase region and partly inside the bulk phase)

$$\rho = V_f \rho (1-\alpha) + V_b \rho_L$$

Control volume C (completely inside the bulk phase)

$$\rho = \rho_L$$

Fig. II.2. The continuum approach used to define the density distribution in the calculation domain.

transmitted across the cavity surface essentially translates into the bulk phase liquid recirculation.

To quantify the shear stresses transmitted from the impinging gas to the bulk liquid interms of an appropriate expression, the empirical formula suggested by Zhang and coworkers[21] has been adopted in the present work and the variation of shear stress across the cavity surface represented according to:

$$\tau(r) = \frac{4\, C_a\, Q_g\, \mu_g}{K\, \pi^{1/2}\, l_o\, d^2} \exp\left[-\left(\frac{r}{3C_r l_o}\right)^2\right] \quad \ldots(II.16)$$

in which l_o, d, Q_g represent the key injection parameters, while C_a, C_r, K are empirical constants (viz., see nomenclature). On the basis of equation (II.16), the axial and the radial components of the shear stress at various locations on the cavity surface have been estimated (by resolving $\tau(r)$ into two mutually perpendicular stress components) and considering relevant area, shear layer thickness etc., the corresponding specific volume shear forces (viz., $F_{s,z}$ and $F_{s,r}$) estimated and added to the axial and radial direction momentum/motion equations as the representative body forces imposed by the top gas injection system (viz., equations (II.3) and (II.5)).

To correlate $F_{s,r}$ and $F_{s,z}$ (the specific volume shear force components, see equations (II.3) and (II.5)) with the shear stress $\tau(r)$, the parabolic cavity surface has been idealised interms of several line segments as illustrated in Fig.II.3. Furthermore, for each line segment, a characteristic radial distance (r) has been chosen (this essentially corresponds to the distance of the geometric centre of the line segment from the axis of symmetry) and the shear stress estimated via equation (II.16). Assuming the shear stress to be

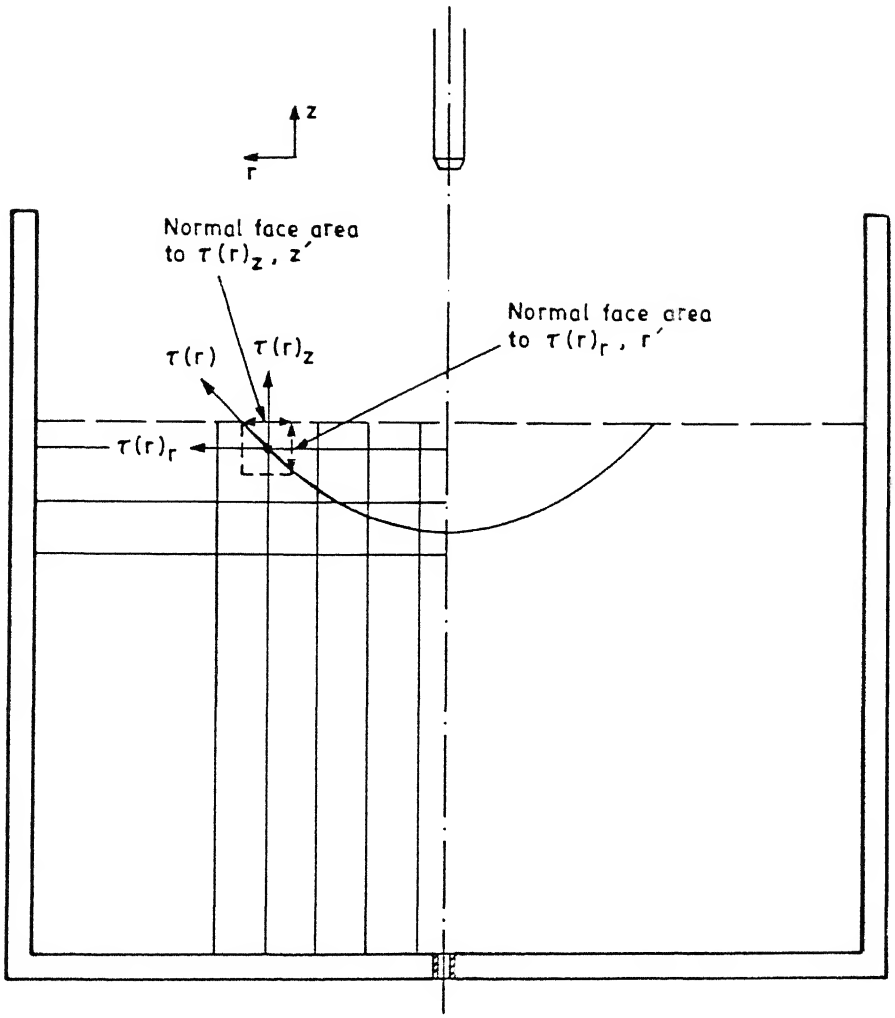

Axial component of shear force = $z'\tau(r)_z$
Radial component of shear force = $r'\tau(r)_r$

Fig. II.3. Segmentised cavity contour and the procedure adopted to evaluate components of shear force / stress at any point on the cavity surface.

prevalent over the entire line segment, the two mutually perpendicular stress components (viz., along the z and the r axes respectively) have been derived, multiplied by the corresponding normal area (viz., see Fig.II.3) and added directly to the axial and the radial direction momentum equations as the required specific volume body forces (= $F_{s,z}$ or $F_{s,r}$ in equations (II.3) etc.). To this end an appropriate shear layer thickness has been assumed (see also later).

II.5 The Boundary Conditions

The boundary conditions applied to the numerical solution of the set of partial differential equations (viz., equations (II.1) through (II.10)) are:

(i) At the axis of the symmetry (r=0 , 0 < z < L)

$$v = 0$$

$$\frac{\partial u}{\partial r} = 0 \; ; \quad \frac{\partial k}{\partial r} = 0 \text{ and } \quad \frac{\partial \varepsilon}{\partial r} = 0$$

(ii) At the free surface of the liquid (z=L, 0 < r < R)

$$u = 0$$

$$\frac{\partial v}{\partial z} = 0 \; ; \quad \frac{\partial k}{\partial z} = 0 \text{ and } \quad \frac{\partial \varepsilon}{\partial z} = 0$$

and at the side walls (r = R, 0<z<L) and bottom surface (z=0, 0<r<R)

$$u=0, \quad v=0, \quad k=0 \text{ and } \varepsilon=0$$

Close to the vicinity of the rigid boundaries (viz., the walls and the bottom surface) where variations in the flow properties are steep, the momentum (u and v) and the scalar (k and ε) fields have consequently been modelled using the routine wall functions[22] (e.g., logarithmic

law of wall for the parallel to wall velocity component etc.). These have been illustrated via Fig.II.4.

II.6 Numerical Solution Procedure

Since F_B, $F_{s,z}$ and $F_{s,r}$ can be conveniently estimated from the procedures outlined already in sections II.3 and II.4, it is therefore readily apparent that the five principal differential equations (viz., equations (II.1), (II.2), (II.4), (II.6) and (II.9)) together with their appropriate boundary conditions (viz.,section II.5) can in principle be solved for the five dependent variables u, v, p, k and ε.

Thus to numerically solve the set of partial differential equations represented by equation (II.1) through (II.10) together with the associated boundary conditions and the auxilary relations, a control volume based finite differnce procedure[23] has been adopted in the present work. In this, the flow domain has been discretized into a number of non-overlapping control volumes. and the governing equations integrated around all such control volumes (staggered control volumes have been considered for the two velocity components) to result into a system of algebric equations, which for any general variable Ø, may be represented according to:

$$A_p \emptyset_p = A_E \emptyset_E + A_W \emptyset_W + A_N \emptyset_N + A_S \emptyset_S + S_c \qquad (II.17)$$

in which, A_p is the centre point coefficient (see Fig. II.5) while A_E, A_W, A_N, A_S are the neighbour point (2 dimensional) coefficients, representing the combined influences of fluid convection and diffusion. Further, S_c represents the positive component of the source

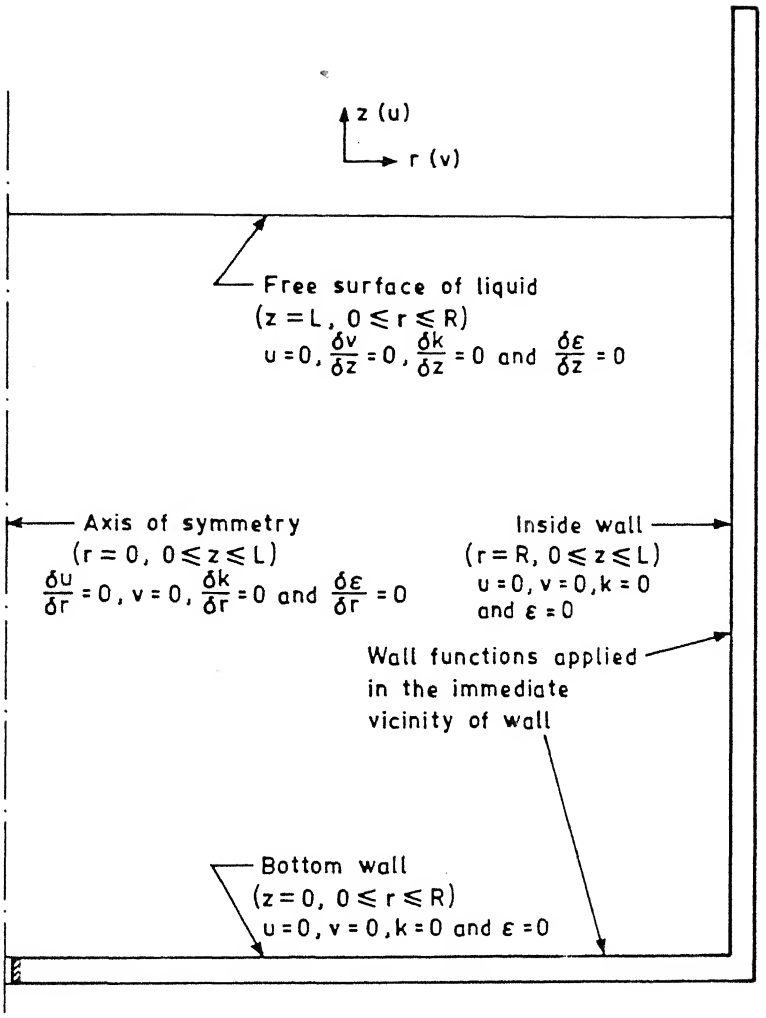

Fig. II.4. Representation of the various boundary conditions applied to the numerical solution of the governing partial differential equations.

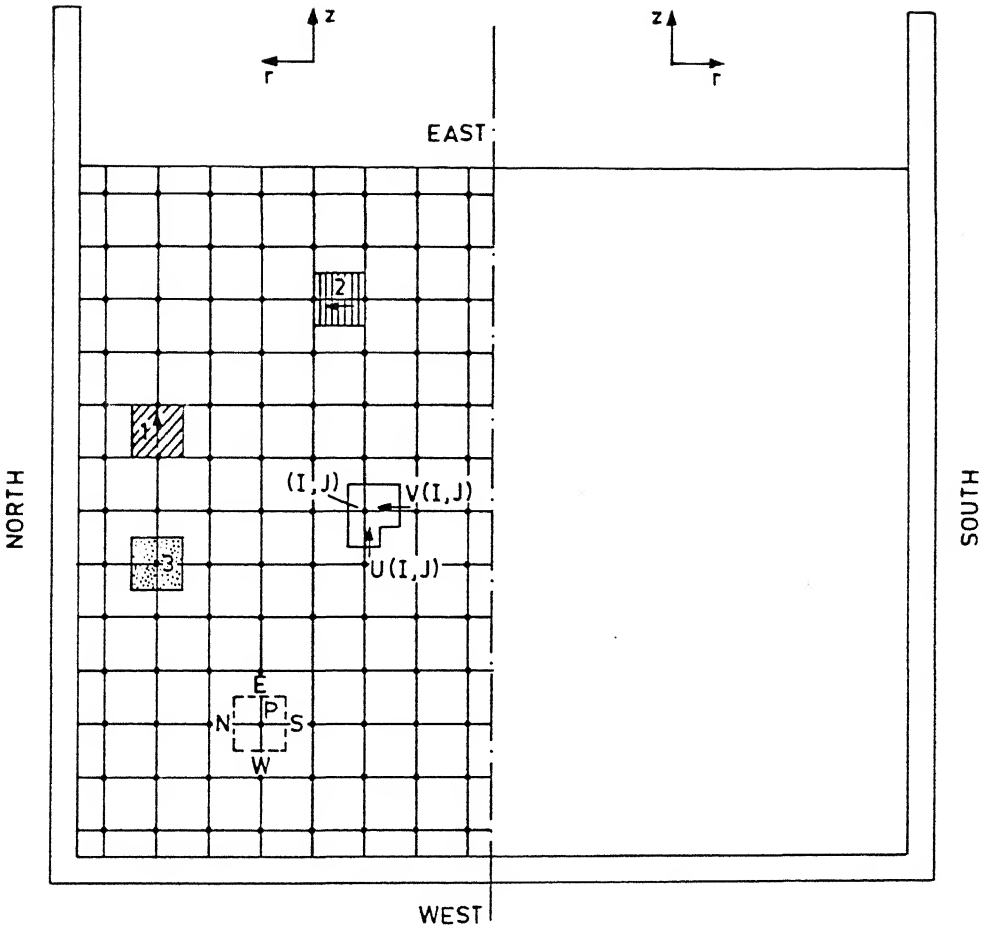

Fig. II.5. Various types of control volumes and the staggered grid system applied to the present numerical solution scheme.

1. u Control volume 2. v Control volume
3. Scalar (k, ε, p) control volume

term, (viz., of S_u, S_v etc. see equation (II.3) for example) while the corresponding negative component has been embodied in the expression of A_p, the centre point coefficient. The set of algebric equations thus derived have been solved via the Tri-diagonal Matrix Algorithm, incorporating a line by line solution technique. The nonlinearity and coupling involved in the algebric equations (these follow from the governing partial differential equations) have been taken care off by adopting to an iterative calculation procedure. Hence, a sequential rather than a simultaneous solution procedure has been embodied in the present calculation scheme.

The pressure-velocity interlinkage in equations (II.1) through (II.5) have been solved by an implicit finite differnce procedure refered to as SIMPLE[24] (Semi-Implicit Method for Pressure Linked Equations). For analysis of the gas-liquid region, the GALA[25] technique (the Gas And Liquid Analyser) was incorporated into the SIMPLE procedure. In this, the physical properties of the fluid mixture in a cell in the two phase region has been averaged on a volumetric basis(see Fig.II.2) This required the conventional mass continuity equation to be replaced by a volume continuity equation, (viz., equation (II.1)) such that volume of fluid entering a volume element equals the total volume of fluid leaving the control volume.

Since an iterative calculation procedure has been adopted, a convergence criterion (Normalised Absolute Residual Source < 0.005)has been set on all the variables (see also later), and calculations were carried out till NARS (Normalised Absolute Residual Source) value for u, v, k, ε and volume continuity all fell below this stipulated value.

II.7 The Computer Program

The numerical solution procedure outlined in the preceeding section refers to a modified version of the popular TEACH-T computer program, used extensively by Mazumdar[8] to underscore the hydrodynamics of ladle gas injection operations. In the present investigation, the modified version of the TEACH-T[8] code has been applied incorporating several other additional modifications /improvements. These for example include,

(i) adaptation to an axisymmetric submerged as well as to an impinging gas jet system through incorporation of various force components (e.g., F_B, $F_{s,z}$ and $F_{s,r}$ into the computational procedure),

(ii) prescription of the density field in the flow domain via the GALA procedure,

(iii) incorporation of different differencing schemes (upwind, exoponential etc.) for calculation of combined convection and diffusion fluxes (viz., the coefficients A_E, A_W etc. in equation II.17)

and finally,

(iv) a procedure (based on the cell porosity method[26]) incorporated to exclude the cavity volume from the domain of calculation.

The latter modifications will be discussed elaborately in the subsequent sections. The flow circuit of the computer program applied to the present investigation has been illustrared in Fig. II.6.

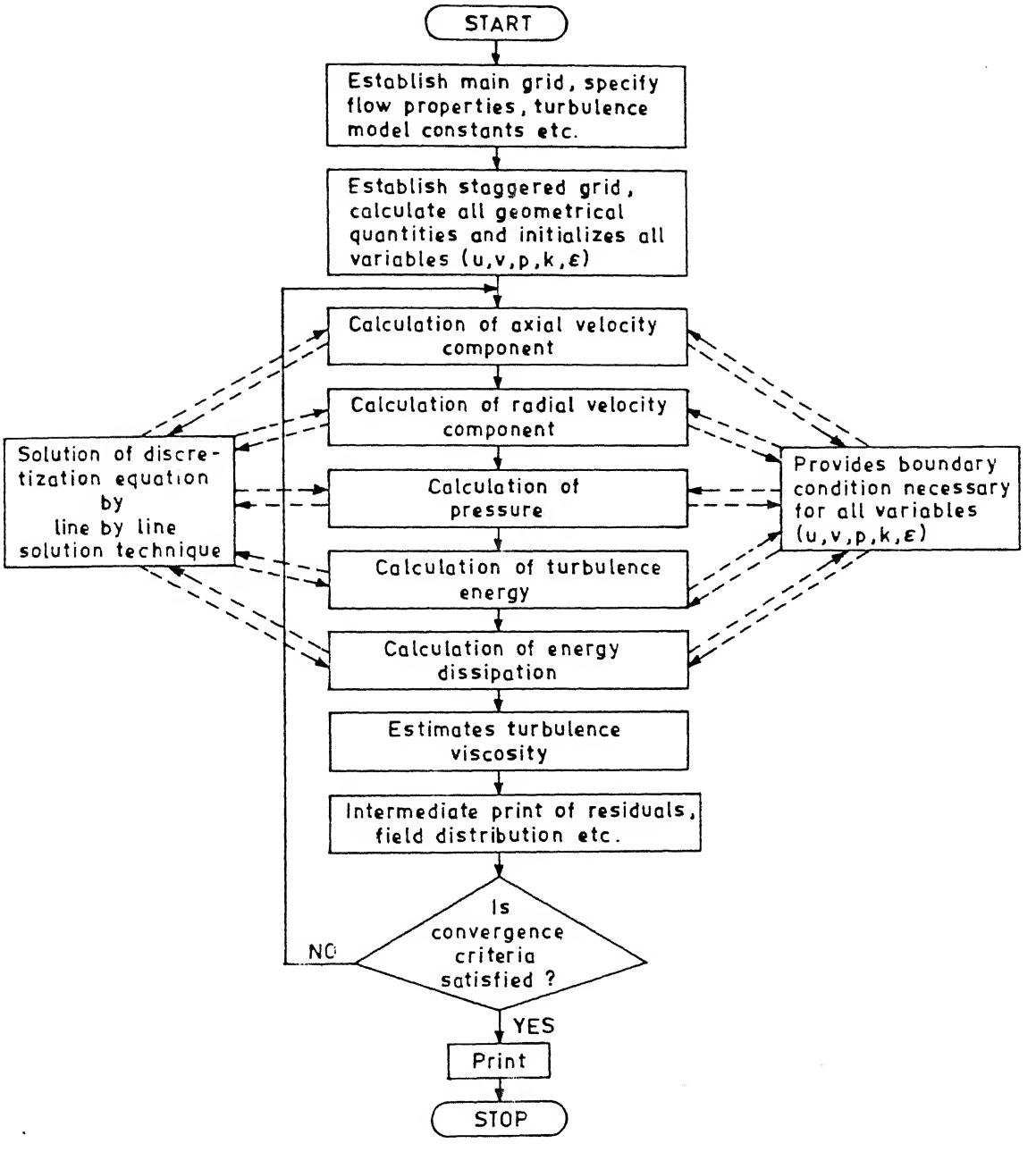

Fig. II.6. Flow sheet of the TEACH-T computer program.

CHAPTER III

RESULTS AND DISCUSSION

III.1 Analysis Of Sources Of Error In The Computed Results

To assess the validity of predicted results from the mathematical model outlined in the preceeding chapter, comparisons between theoretical estimates and experimental measurements are essential. However, prior to any comparisons it is important to ascertain that minimum numerical inaccuracies are involved in such calculated results. For a given set of equations and boundary conditions, the extent of assosiated error in the computed results is expected to depend upon several numerical parameters. These include,

(a) the maximum allowable residual source (e.g.,the convergence criterion),

(b) the distribution of grid systems in the flow domain

and

(c) the differencing schemes applied to estimate the convection and diffusion fluxes embodied in the discretization equations (e.g., the coefficients A_p, A_N, etc.).

It is important to recognise here that these numerical parameters simultaneously affect the accuracy of results as well as the assosiated computation times, CPU. Consequently, an optimum balance between accuracy and CPU time has to be considered for any effective error analysis.

III.1.1. The influence of residual source sum values on computed result

Since an iterative calculation procedure has been adopted to numerically solve the governing partial differential equations, a

convergence criterion needs to be specified. To this end, a residual source, R_L, defined as

$$R_L = |\sum A_{nb} \phi_{nb} + S_c - A_p \phi_p| \quad \ldots(III.1)$$

has been estimated at each nodal point and added up over the entire flow domain for each individual variable involved (viz., u,v,K,ε etc.). Obviously, when the discretization or the finite difference equations are completely satisfied, R_L will be zero for all equations. However, since this requires an extremely large computation time to be achieved, a suitable convergence criterion is required to be specified so that the value of $\sum \sum R_L$ ($\sum \sum$ indicates summation over the two dimensional flow domain) be less than a certain small number. However, smaller is this allowable residual source value, the larger would be the computation time. Hence, it is desirable to find out an optimum allowable residual source value for the present problem.

To assess the sensitivity of computed results to the value of residual source, R_L, calculations were carried out for a submerged gas injection configuration (F_B is finite, $F_{s,z}$ and $F_{s,r}$ are respectively zero in equations (II.3) and (II.5)) corresponding to the experimental conditions of Mazumdar et al.[27] (e.g., $Q=1.667\times10^{-5}$ m^3/s). These are shown in Table III.1 for ready reference. A relatively large number of grid system (viz.,15x10) have been applied to encompass the flow domain (L=0.21m and R=0.15m) providing an effective grid spacing of approximately 20mm in either direction. Further, the hybrid differencing scheme[23] has been applied to estimate the convection and the diffusion fluxes (viz., the coefficients A_p, A_N etc.).

Table III.1 Experimental conditions of different investigators used in the computation of results presented in Figs. III.1 through III.5.

	Experimental conditions of		
	Mazumdar and Guthrie[27]	Castillejos and Brimacombe[30]	Lehner and co-workers[13]
Bath height, m	0.21	0.4	1.08
Radius of the vessel, m	0.15	0.25	0.76
Diameter of the nozzle, m	1.5×10^{-3}	6.35×10^{-3}	———
Gas flow rate, m^3/s	(1.67×10^{-5}, 3.33×10^{-5} and 5.0×10^{-5})	3.6395×10^{-4}	1.667×10^{-3}

The predicted radial distribution of vertical velocity component at two different depths in the water model has been shown in Fig. III.1 for three different values of $\sum\sum R_L$ (viz.,0.001, 0.005 and 0.025). This appears to suggest that a reasonable value for the sum of the residual source is approximately $5x10^{-3}$ and further lowering of this value does not lead to any improved accuracy in the predicted results. However, if a sum of residual source value of approximately 0.025 is applied in the numerical calculation procedure, significant accuracy in predicted results appears to be lost. Consequently, for all subsequent calculations reported in this thesis, an allowable sum of residual value equivalent to $5x10^{-3}$ has been applied. Towards this, it is important to note here that in numerous equivalent previous studies (see for example reference 4), the selection of an appropriate convergence criterion has neither been adequately considered nor explicitly specified. In addition, usage of widely different convergence criteria has also been noted[7,21]. This is particularly critical when comparisons between theory and experiments are to be made, since computed results depend considerably on such criterion.

III.1.2 The influence of nodal configurations on computed results

The derivation of the discretization or the finite difference equations from the governing differential equations require numerous assumptions to be invoked (viz.,the mode of variation of the dependent variables between two nodal points etc.), and consequently, predicted results, as one would normally anticipate, would be sensitive to the nodal configurations applied to the numerical solution scheme. However, it is well known that in the limit of a very large number of grid network, these assumptions and their resultant

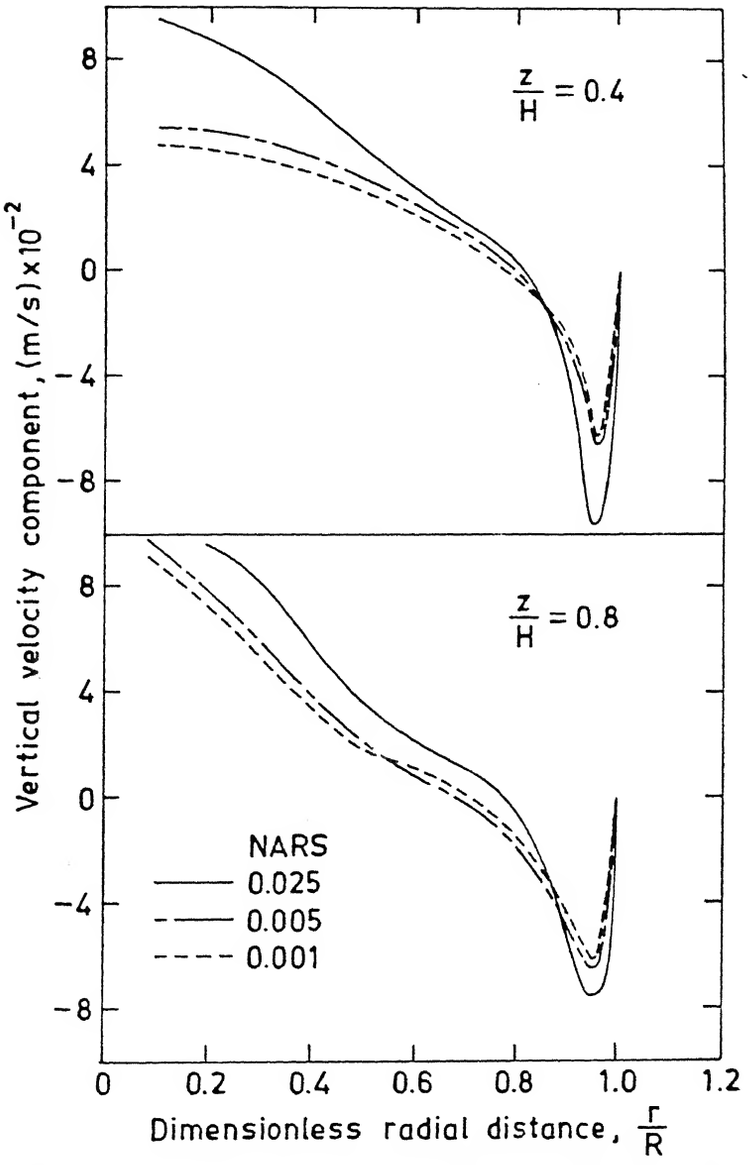

Fig. III.1. Sensitivity of computations to the choice of residual (NARS) values illustrating the radial variation of the vertical component of flow for three typical NARS values ($Q = 1.67 \times 10^{-5} m^3/s$, $R = 0.15$ m, $L = 0.21$ m, 15×10 grid system).

influence on calculated results tend to be insignificant and therefore, the numerical predictions appear to approach to the exact solution (in situations where such solutions can be derived). Consequently, it is essential to establish grid independent solutions prior to any comparison between theory and experiments. Towards this,clearly an optimum nodal configuration for each individual problem has to be known (Indeed, a more meaningful parameter would be the grid spacing rather than the number of grids, since the former would allow one to deduce the required number of grids that would lead to grid independent results for any domain size).

To test these, flows in a submerged gas injection system in a cylindrical ladle (L=0.21m and R=0.15m) has been modelled mathematically by applying three different grid configurations viz., 10x7, 15x10 and 17x12 grid systems respectively. While, the hybrid differrencing scheme has been applied[23], an allowable sum of residual source equal to 0.005 has been considered in the calculation procedure. A comparison among numerically predicted radial distribution of vertical velocity component at two different depths in the water model is shown in Fig. III.2. This indicates that both 15x10 and 17x12 grid systems produce results that are practically equivalent. Consequently, predictions via a 15x10 grid system can be considered to be essentially grid independent. On the basis of this, grid spacing of approximately 20mm have been applied in either directions in all subsequent computations. It is to be noted here that the 10x7 grid system leads to results considerably different to those deduced from the two other nodal configurations.

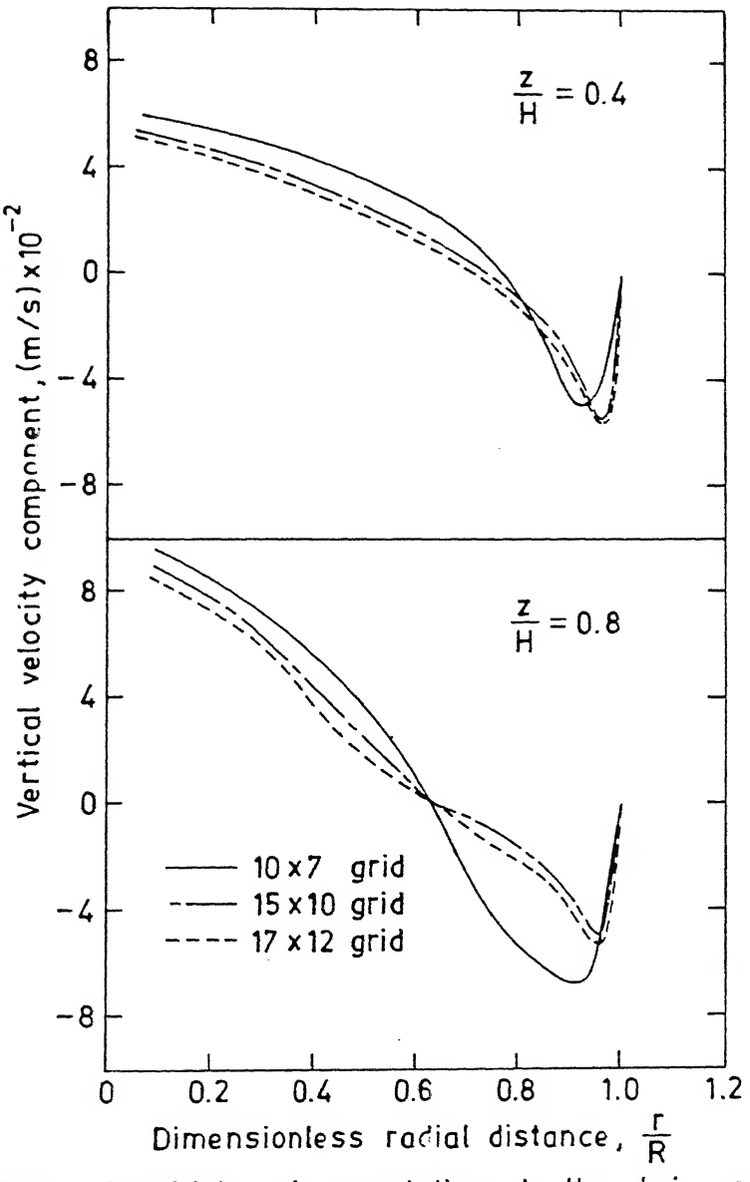

Fig. III.2. Sensitivity of computations to the choice of nodal configurations illustrating the radial variation of the vertical component of flow for three different grid systems ($Q = 1.67 \times 10^{-5}$ m^3/s, $R = 0.15$ m, $L = 0.21$ m, NARS = 5×10^{-3})

III.1.3 The influence of differencing schemes on computed results

As mentioned in the previous chapter, the discretization equations embody coefficients (A_P, A_N, A_S etc.) that represent the combined influences of fluid convection and diffusion processes. To estimate these coefficients (e.g., the convection and the diffusion fluxes) from the relevant velocity and diffusion coefficient values, several schemes can in principle be applied and these, for example, include :

(1) the central differencing scheme

(2) the upwind differencing scheme

(3) the hybrid differencing scheme

(4) the exponential differencing scheme

and

(5) the power law differencing scheme

It is to be mentioned here that except for the central differencing scheme, all others are known to produce physically realistic solution for both high and low Reynolds number flows[23]. Consequently, the central differencing scheme has not been considered in the present analysis because of such obvious limitations.

Since these differencing schemes incorporate various assumptions (for example, the upwind scheme ignores diffusion effects for all values of Peclet number etc.[23]), consequently, numerically predicted results are likely to be a function of the differencing schemes employed. Thus to test the sensitivity of computed results to the choice of the differencing schemes, flow calculations were performed via all the four schemes corresponding to the experimental conditions of Mazumdar et al.[27] (viz., those used in the computation

of Figs. III.1 and III.2 (see Table III.1)) and the predicted radial distribution of vertical velocity component at two different depths in the model has been compared in Fig. III.3. This clearly indicates that the differencing schemes employed have practically negligible influence on the overall accuracy of predicted results. It is to be mentioned here that a 15x10 grid system together with an allowable residual source sum of 0.005 have been applied to derive the results presented in Fig. III.3.

Figure III.3 further illustrates that diffusive momentum transfer in such systems is relatively less important, since results of the upwind and the rest of the differencing schemes are very similar. Such computed results therefore, appear to indicate that flows in metallurgical ladles are largely dominated by the inertial forces and that viscous effects (both molecular and turbulent) play insignificant roles in affecting the overall flow pattern induced. This is clearly substantiated from the results presented in Table III.2, which indicate that the predicted mean speed of liquid recirculation via all the four differencing schemes are practically identical (maximum variation ± 15%) and eqivalent to those observed experimentally by Mazumdar et al.[27].

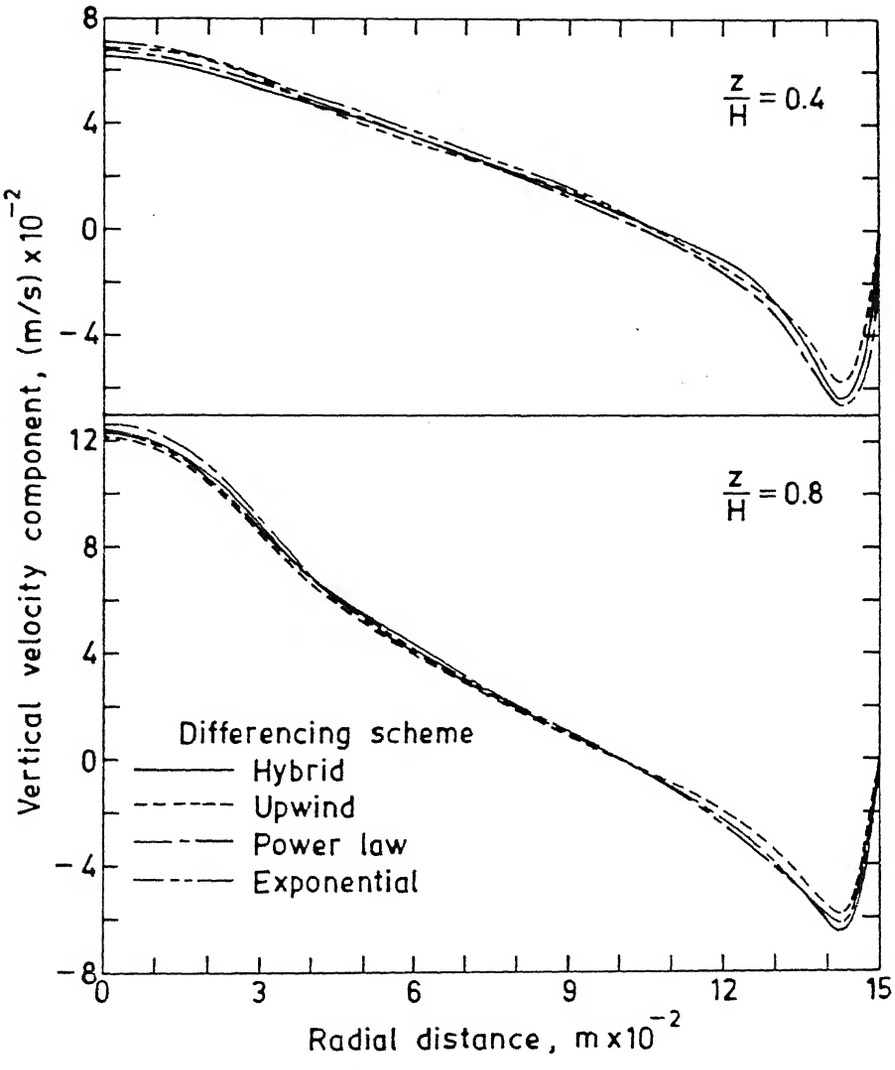

Fig. III.3. Sensitivity of numerically predicted vertical velocity component in a water model of a gas stirred ladle[27] illustrating the influence of differencing scheme employed on predicted results.

Table III.2 Theoretically predicted mean speed of liquid recirculation via various differencing schemes and their comparison with experimental measurements of Mazumdar et al.[27]

Differencing scheme	Mean speed of liquid recirculation(mm/s)	
	Numerical predictions	Experimental values
Upwind	37.13	
Hybrid	40.07	
Power law	40.07	34.0
Exponential	45.32	

III.2 Evaluation Of Calculation Procedures For Modelling Of The Bottom Gas Injection Process

In the present study, as has been mentioned already in the preceeding chapters, the Eulerian quasi-single phase approach has been adopted to model the bottom gas injection process. Because of the relative ease with which such computational procedure can be applied, the quasi-single phase modelling has been widely popular and therefore, several versions of the procedure are available in the literature. In essence, the quasi-single phase modelling procedure is applied via *a prior* specification of *the* geometry as well as the gas volume fraction, α, in the plume. Since the gas volume fraction specified within the plume region plays key role in determining the overall flow field in such buoyancy driven systems, therefore, the various procedures available for gas volume fraction calculation are required to be carefully examined. To this end, any comparison among these calculation procedures has so far not been attempted, and consequently it is necessary to assess the adequacy of these by evaluating their relative performances, so that the most accurate approach can be identified and adopted to model the submerged gas injection system in a combination blown reactor.

III.2.1 Prediction of flow parameters and average speed of bath recirculation via different procedures and their comparisons with experimental measurements

To estimate the gas volume fraction, α, in the rising two phase plume, different group of investigators have adopted widely varying concepts and based on these, four distinct types of

computational procedures have so far emerged. These are discussed below in detail.

III.2.1.a The procedure adopted by Szekely and coworkers[3,4]

Szekely and coworkers[3,4] through momentum balance over a small volume element in the plume region proposed an ordinary differential equation for estimation of the average plume rise velocity viz.,

$$\frac{dU_z}{dz} + \frac{U_z}{z} = \frac{\pi Q_g g}{2 (\tan \lambda)^2 u_z^2 z^2} \quad \ldots(III.1)$$

in which, U_z is the average rise velocity at any axial station, z.

The boundary conditions considered applicable to equation(III.1) is

$$z=h_0,\ U_z=U_0$$

The average rise velocity has been further related to the gas voidage α according to:

$$\alpha(z) = \frac{Q_g - \pi r_c^2 \alpha(1-\alpha) U_s}{2\pi \int_0^{r_c} U_z\, r\, dr} \quad \ldots(III.2)$$

in which, U_s is the slip velocity and is considered to be synonymus to the rise velocity of a characteristic single bubble in the quiscent liquid[5] and is deduced from a knowledge of the average bubble diameter in the system viz.,

$$U_s \cong U_B = 1.08\left(\frac{gd_B}{2}\right)^{1/2} \quad \ldots.(III.3)$$

Further, U_0 in the boundary condition is the superficial gas velocity and is deduced from :

$$U_0 = \frac{Q_g}{\pi r_0^2} \quad \ldots\ldots(III.4)$$

The void fractions, α, thus obtained are clearly cross-sectional average void fractions. It is apparent that once the plume geometry is known and the void fraction distribution within the plume established via equations (III.1) and (III.2), the equations of motion can be readily solved to yield the distribution of flow variables in the entire calculation domain.

III.2.1.b The procedure adopted by Sahai and Guthrie[5,6]

Sahai and Guthrie used an alternative concept to estimate the volume fraction distribution in the rising plume. Through detailed hydrodynamic considerations, the authors[5,6] suggested a simple, yet effective formula for estimation of rise velocity in the two phase plume according to :

$$U_p = 4.4 \frac{Q^{1/3} \; L^{1/4}}{R^{1/3}} \quad \ldots\ldots(III.5)$$

and related the plume rise velocity to the gas volume fraction via the volume continuity principle :

$$\alpha_{av} = \frac{Q \frac{L}{U_p}}{\pi r_{av}^2 L} \quad \ldots\ldots (III.6)$$

in which, r_{av} refers to average radius of the plume, which is equal to $(1/\sqrt{3})r_{eye}$ (e.g., the corresponding radius at the mid bath depth). In equation (III.6) no consideration of bubble slippage has been given and further, the gas volume fraction has been considered to be

spatially uniform over the entire volume of the two phase plume.

III.2.1.c The procedure adopted by Mazumdar and Guthrie[28]

Mazumdar and Guthrie[28] modified the procedure adopted by Sahai and Guthrie[5,6] to estimate the gas volume fraction in the plume. These authors[28] adopted the macroscopic plume model of Sahai and Guthrie (viz., equation (III.4)), and deduced the gas volume fraction in the plume from the following relationship :

$$\alpha(z) = \frac{Q_g - \pi r_c^2 \alpha(1-\alpha) U_s}{2 \pi U_p \int_0^{r_c} r \, dr} \quad \ldots.(III.5)$$

Clearly, the value of U_p is constant throughout the two phase plume and therefore α, the cross-sectional average void fraction is a function of z only. Equation (III.5) is different from equation (III.2) since instead of U_z, U_p, a constant plume rise velocity has been used. The authors[28] justified the use of a constant rise velocity rather than a variable one (viz., U_z) in equation (III.5), since experimental plume rise velocity deduced by Lehner et al.[13] were found to be independent of the axial distance. The procedures adopted by Guthrie and coworkers[5,6,28] like those of Szekely et al.[3,4] also require *a prior* specification of the plume geometry.

III.2.1.d Zhang and coworkers[21] formulation for estimation of gas void fraction in the plume

Zhang et al.[21] proposed a new approach to estimate the gas volume fraction within the plume. For the three previous approaches outlined earlier, the geometry of the plume has to be specified *a priori*. In contrast, however, Zhang et al.'s formulation does not

require prior specification of the two phase domain and instead, the gas volume fraction within the flow domain is deduced from the following empirical relationship:

$$\alpha(r,z) = \alpha_m \exp\left[- \frac{r^2}{C_g^2 (H-z+h_o)^2} \right] \quad ...(III.7)$$

in which, α_m represents the void fraction at the axis of symmetry and is estimated from :

$$\alpha_m(z) = C_t \, Q^{2/3} \left[\frac{\rho_L}{(\rho_L - \rho_g)g} \right]^{1/3} (H-z+h_o)^{-3/5} \quad ..(III.8)$$

In equations (III.7) and (III.8), C_g, C_t represents two empirical dimensionless constants which were assigned to values 0.12 znd 9.1 respectively.

To assess the relative accuracy of predictions via the four different approaches outlined above as well as their adequacy with reference to the mathematical modelling of submerged gas injection systems, flow calculations were accordingly carried out corresponding to the experimental conditions reported earlier by Mazumdar et al. (see Table III.1).

Towards this,to solve equation (III.1) and hence to deduce the gas volume fraction in the plume a computer program incorporating a fourth order Runga-Kutta method[29] has also been developed. This is presented in the Appendix. The plume dimensions were estimated from the previously published experimental data and further a bubble diameter of 10mm has been considered to deduce the slip velocity. Incorporating the $k-\varepsilon$ turbulence model with each of the previously mentioned gas volume fraction calculation procedures, the distribution of the axial

(u) and the radial (v) velocity components in the flow domain were deduced through the solution of relevant momentum balance equations and from these, the average or mean speed of liquid recirculation, $\bar{U}$, estimated as :

$$\bar{U} = \frac{\int_0^L \int_0^R |(u^2+v^2)^{1/2}| \, 2\pi r \, dr \, dz}{\int_0^L \int_0^R 2\pi r \, dr \, dz} \quad \ldots(III.9)$$

The above integration has been carried out numerically adopting the Eulerian integration procedure(viz., assuming $|(u^2+v^2)^{1/2}|$ to prevail over a control volume).

Numerically predicted mean speed of liquid recirculation thus obtained have been directly compared with the corresponding experimental measurements of Mazumdar et al.[27] derived for three different gas flow rates in a water model (L=0.21m and R=0.15m) of a gas stirred ladle system. It is to be mentioned here that the kinetic energy of the incoming gas has been ignored for the flow calculation as a first approximation, since this is significantly lower (typically about 10% or less) in comparison to the potential energy afforded by the gas rising through the liquid.

The comparison between theory and experiments illustrated in Table III.3. clearly indicates that the hydrodynamics of the submerged gas injection system is adequately represented via the procedure suggested by Mazumdar and Guthrie[28]. It is further apparent that Sahai and Guthrie's prescription of gas voidage leads to a higher rate of bulk fluid recirculation. This can be anticipated since in their calculation procedure[5,6] bubble slippage has not been considered.

Table III.3 Experimentally measured mean speed of liquid recirculation[27] and their comparison with those estimated theoretically to illustrate the sensitivity of prediction to the choice of the gas volume fraction calculation procedures.

Gas flow rate, m^3/s	Computational procedures for gas voidage calculation	Numerically predicted mean speed of bath recirculation, mm/s	Experimentally measured mean speed of bath recirculation, mm/s
0.166×10^{-4}	a) Szekely and co-workers[3,4]	28.18	34.0
	b) Mazumdar and Guthrie[28]	31.43	
	c) Sahai and Guthrie[5,6]	40.07	
	d) Zhang et al.[21]	7.215	
0.333×10^{-4}	a) Szekely and co-workers[3,4]	29.22	45.45
	b) Mazumdar and Guthrie[28]	46.27	
	c) Sahai and Guthrie[5,6]	54.34	
	d) Zhang et al.[21]	11.69	
0.5×10^{-4}	a) Szekely and co-workers[3,4]	30.22	53.42
	b) Mazumdar and Guthrie[28]	55.66	
	c) Sahai and Guthrie[5,6]	71.95	
	d) Zhang et al.[21]	15.29	

With reference to the results shown in Table III.2 it is also important to recognize here that Zhang et al's formulation, in contrast to the three other equivalent computational procedures, provides significantly lower estimates of mean speed of liquid recirculation.

III.2.2 Estimates of gas volume fractions within the plume and their comparison with experimental measurements of Castillejos and Brimacombe[30]

Extensive measurements of gas volume fractions within the rising two phase plume in water models of gas stirred ladles have been recently reported by Castillejos and Brimacombe[30]. To assess the adequacy of the theoretically predicted voidage values deduced via the four different procedures outlined in the preceeding section, the gas volume fraction distribution within the rising plume were estimated corresponding to the experimental measurements of Castillejos and Brimacombe (see Table III.2).

The experimental centreline gas voidages have been compared directly in Fig III.4 against the corresponding estimates derived via each of the four calculation procedures assuming a bubble slip velocity of 0.22m/s (this corresponds to a bubble diameter of 10mm). There, it is clearly seen that the procedure suggested by Mazumdar and Guthrie[28] provides the most reasonable estimates of the gas volume fraction distribution in the plume. Similarly, in Fig III.5 the cross-sectional average void fractions deduced via the four calculation procedures have been compared with equivalent experimental observations of Castillejos and Brimacombe[30]. Once again adequacy of the procedure suggested by Mazumdar and Guthrie[28] is readily

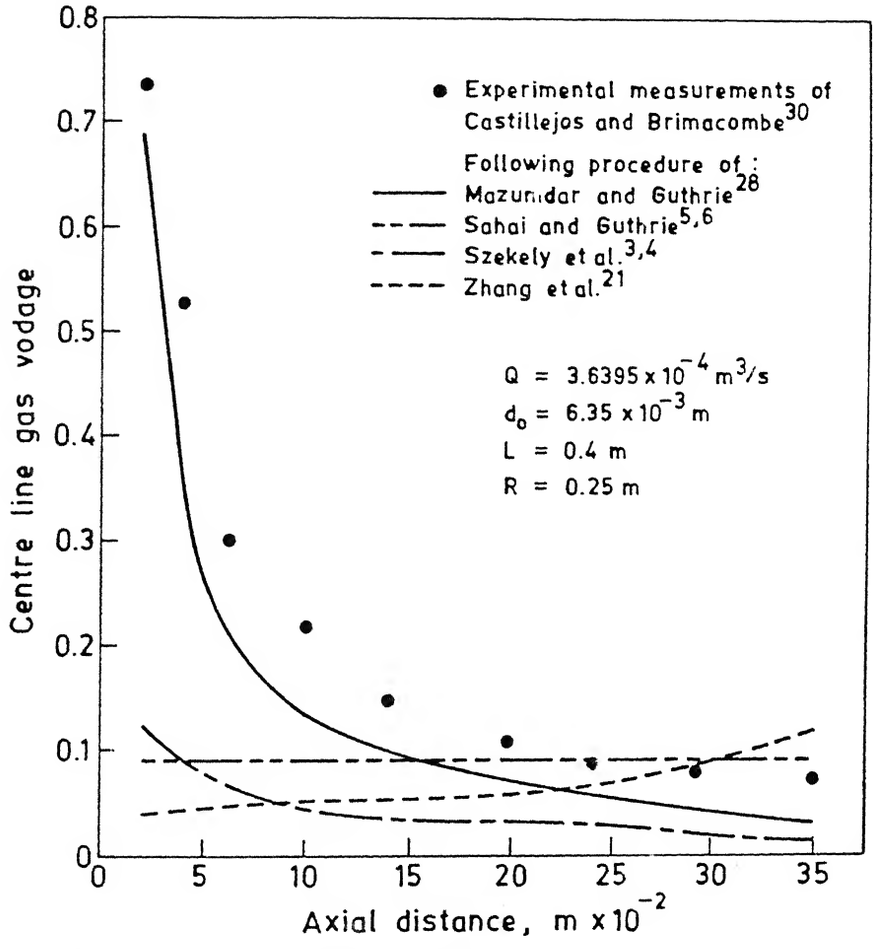

Fig. III.4. Theoretically estimated centre line gas voidages in a water model ladle and their comparison with equivalent experimental measurements

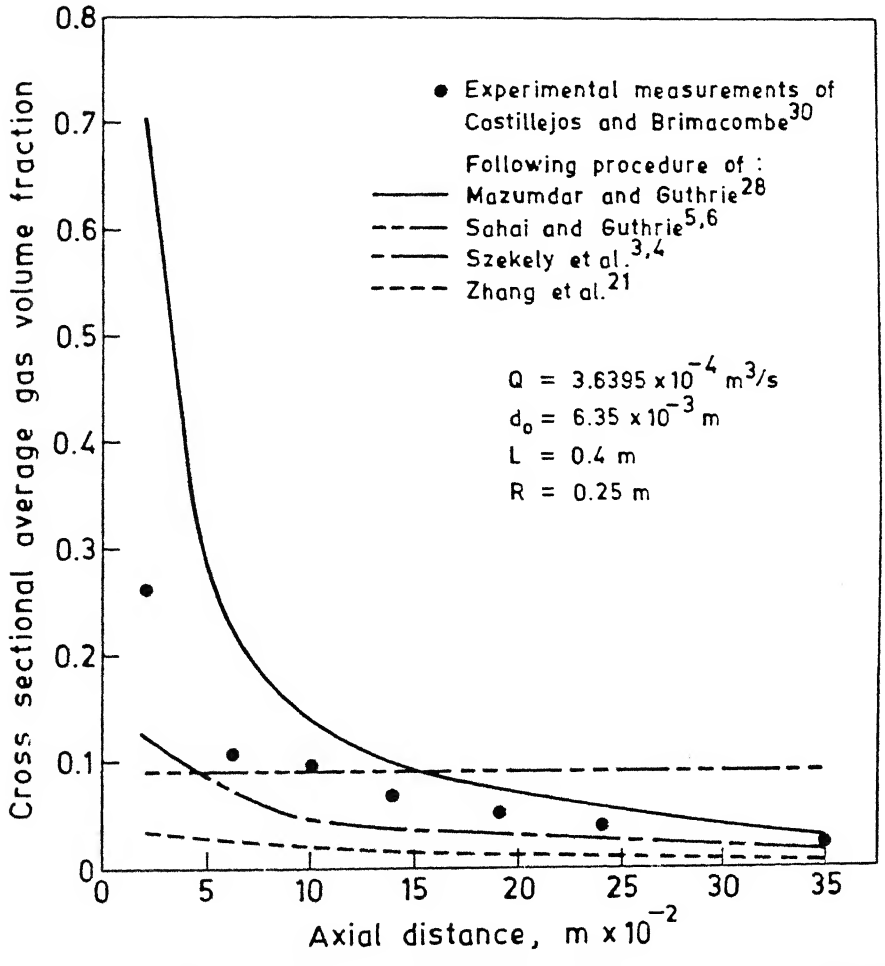

Fig. III.5. Theoretically estimated cross sectional average gas voidages in a water model ladle and their comparison with experimental measurements.

apparent.

Referring to Figs. III.4 and III.5, one also finds that the gas volume fraction deduced via the procedure of Sahai and Guthrie[5,6] is somewhat over estimated along almost 75% of the plume height. Similarly, the void fraction deduced via Szekely et al.'s procedure[3,4] is somewhat smaller than those experimentally observed. In contrast to all these, Zhang et al.'s formula[21] provides estimates of gas voidages that are significantly lower than the experimental values. More important, however, is their[21] estimates of centreline gas voidages that seem to increase with the axial distance, z, which clearly contradicts the experimental findings.

On the basis of the preceeding discussion, one would therefore expect that the hydrodynamics of a submerged gas injection system can be simulated adequately via the calculation procedure suggested by Mazumdar and Guthrie[28]. While one would also expect that Sahai and Guthrie's prescription of α would provide higher rates of bulk recirculation, equivalent procedures of Szekely and coworkers[3,4] as well as that of Zhang and coworkers[21] would produce smaller rates of bulk recirculation in the reactor vessel. Such a trend in predicted results is readily apparent in Table III.2. It is instructive to note here that in all the calculation procedures adopted for the estimation of α, barring the procedure of Zhang and coworkers[21], radial variation of gas voidages in the plume has been ignored[3,4,5,6,28] and hence the cross-sectional average void fraction at any axial distance can be visualised to be identical to the gas voidage at the axis of symmetry (viz.,the centre line). The results presented so far also appear to indicate that such radial variations can be ignored as a first approximation, so far as the

modelling of the bulk phase hydrodynamics is concerned.

III.2.3 Prediction of rise velocity within the plume and their comparison with experimental measurements of Lehner et al.[13]

So far, adequacy of the calculation procedure of Mazumdar and Guthrie[28] has been demonstrated with reference to the estimation of gas voidage distribution in the plume as well as the mean speed of bath recirculation. To assess the appropriateness of the calculation procedure[28] further, particularly with reference to the prediction of rise velocity within the plume region, computations were also carried out corresponding to the experimental conditions of Lehner et al.[13] (these are summarised in Table III.1) and the predicted rise velocity at various axial stations within the bath compared directly in Fig. III.6 with the corresponding experimental measurements[13]. Reasonable agreement between theory and experiments is once again readily apparent. With refernce to the results presented in Fig. III.6, it is to be mentioned here that a slip velocity (U_s) equivalent to 0.4 m/s has been assumed. This corresponds to a bubble diameter of approximately 30mm, which is typical of such water model systems in the regime of the gas flow rates considered.

On the basis of the preceeding discussion, therefore, the calculation procedure adopted by Mazumdar and Guthrie[28] has been applied to represent the bottom gas injection process in the combination blown system.

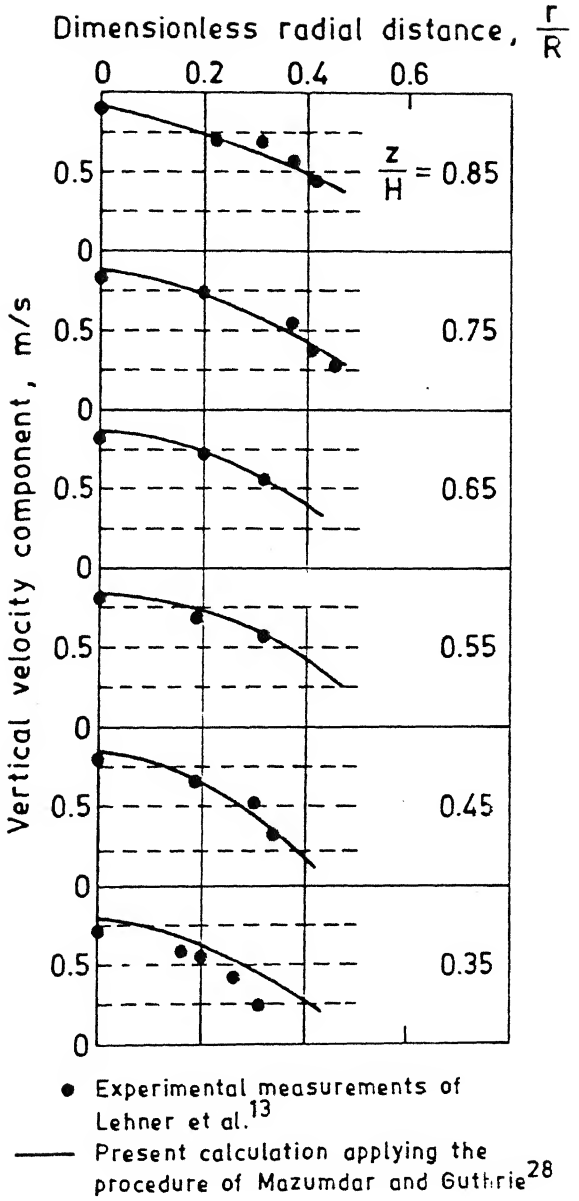

Fig. III.6. Theoretically predicted vertical velocity component within the rising plume and their comparison with experimental measurements of Lehner et al.[13]

III.3 Modelling Of The Top Gas Injection System And Comparison with Experimental Measurements

In the preceeding sections, modelling of the bottom gas injection process has been considered in detail and an adequate mathematical representation for the gas injection induced flow developed. In this section, modelling approaches for the impinging gas jet system currently available in the literature will be discussed and evaluated rigorously. Once the appropriate procedure has been identified, the desired mathematical model for the combination blown system can then be derived by considering these models for the bottom as well as the top gas injection systems respectively.

III.3.1 The shearing forces acting across the cavity surface and its role in driving the bulk phase flow in the top gas injection system

Earlier investigators[17,21] engaged in modelling of flows generated by an impinging gas jet considered that the shearing forces acting across the cavity surfaces is primarily responsible for producing the bulk flow recirculation. These studies, therefore, considered that the gas impinging over the bath surface forms a cavity and as the gas stream flows radially over the cavity surface, the outflowing gas stream drags a layer of fluid through shearing actions and this phenomenon produces the flow recirculation observed in such systems. In accordance with these concepts, therefore, the relevant shearing forces have been estimated from the gas injection parameters (viz.,section II.2.1) and embodied in the axial and the radial direction momentum equations as the appropriate driving body force term. The relationship between the gas injection parameters and the

corresponding shear stress adopted in the present study has been the same as that suggested by Zhang and coworkers[21]. The concepts applied to estimate the required body forces from the empirical expression of shearing stresses[21] have been considered briefly alredy in section II.4.

To assess the effectiveness of the above concept (e.g.,that the flows are essentially driven via the shearing forces) as applied to the modelling of an axisymmetric top gas injection system, an experimental fluid flow study reported earlier on such systems by Jagannathan and coworkers[31] has been considered. These authors[31] reported extensive measurements of flow parameters in a water model of a LD reactor via Laser Doppler Annemometer. The corresponding experimental conditions have been summarised in Table III.4 for ready reference. The configuration of the idealised cavity surface contour with reference to the finite difference grid systems used for the present mathematical representation has been illustrated in Fig.III.7. This shows the segmentised cavity contour, the components of the shearing forces at any location on the cavity surface and the relevant normal area across which the stress components have been assumed to be acting. Further, the shearing forces thus estimated have been assumed to be prelevant over the control volumes lying immediately below the cavity. This implicitly implies that a shear layer thickness equivalent to about a control volume dimension (e.g.,≅ 20mm) has been considered for the present flow calculations. Incorporating adequate expressions for $F_{s,z}$ and $F_{s,r}$ in relevant equations of motion in terms of $\tau(r)$ and the appropriate grid parameters, and further considering $F_B=0$ (see section II.2.1), computations were carried out corresponding to the experimental conditions of Jagannathan et al.[31].

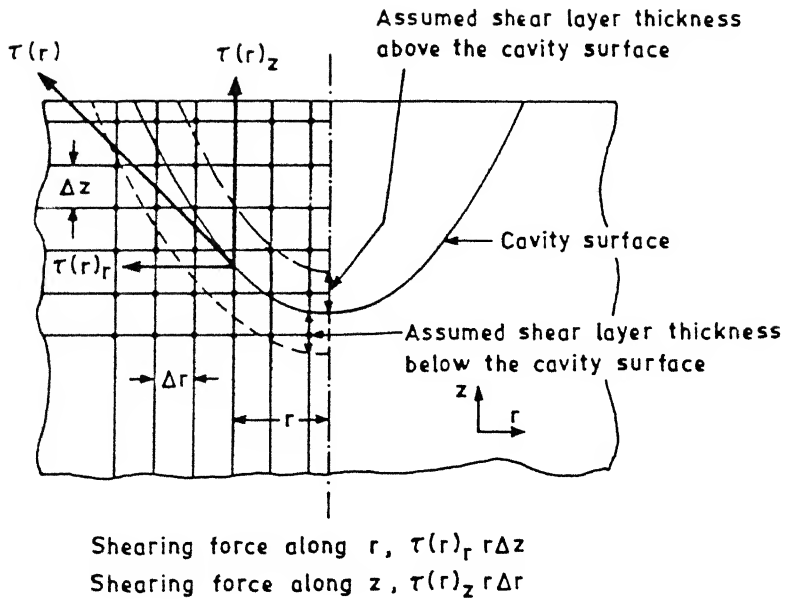

Fig. III.7. The shearing forces acting at a location on the cavity surface and the configuration of the shear layer thickness with reference to the finite difference grid system.

Numerically predicted vertical velocity components at four different depths in the model has been compared directly in Fig.III.8 with the experimental observations of Jagannathan and coworkers. This clearly indicates considerable differences between theory and experiments and the predicted flow is seen to be significantly smaller (by about a factor of 8 or so) than the corresponding experimental values.

This discrepancy between theory and experiments clearly requires some rigorous analysis and to this end the sensitivity of calculations to the value of l_0 (=distance of seperation between the lance nozzle and the bath free surface) must first be assessed, since no value of l_0 has been specified by Jagannathan and coworkers[31]. It is important to note here that calculations reported in Fig.III.8 has been driven by assigning an arbitrary but likely value of 150mm to l_0. Similarly the assumption of a shear layer thickness equivalent to the size of a control volume may also introduce some uncertainity in the numerical predictions.

To evaluate these, sensitivity of flow predictions has been carried out to the choice of values of l_0 and the shear layer thickness. In Fig.III.9, predicted vertical velocity component at two different depths in the model have been compared considering two arbitrary but probable values of the parameter l_0 (=150mm and 220mm respectively). This evidently indicates that predicted results are relatively insensitive to the precise value of l_0 chosen. Similarly, the shear layer thickness has been arbitrarly increased by a factor of two (shear stress assumed to be prelavent over a region that is twice as thick as that considered in the computation of Fig III.8) and the numerical predictions repeated for the conditions of computations

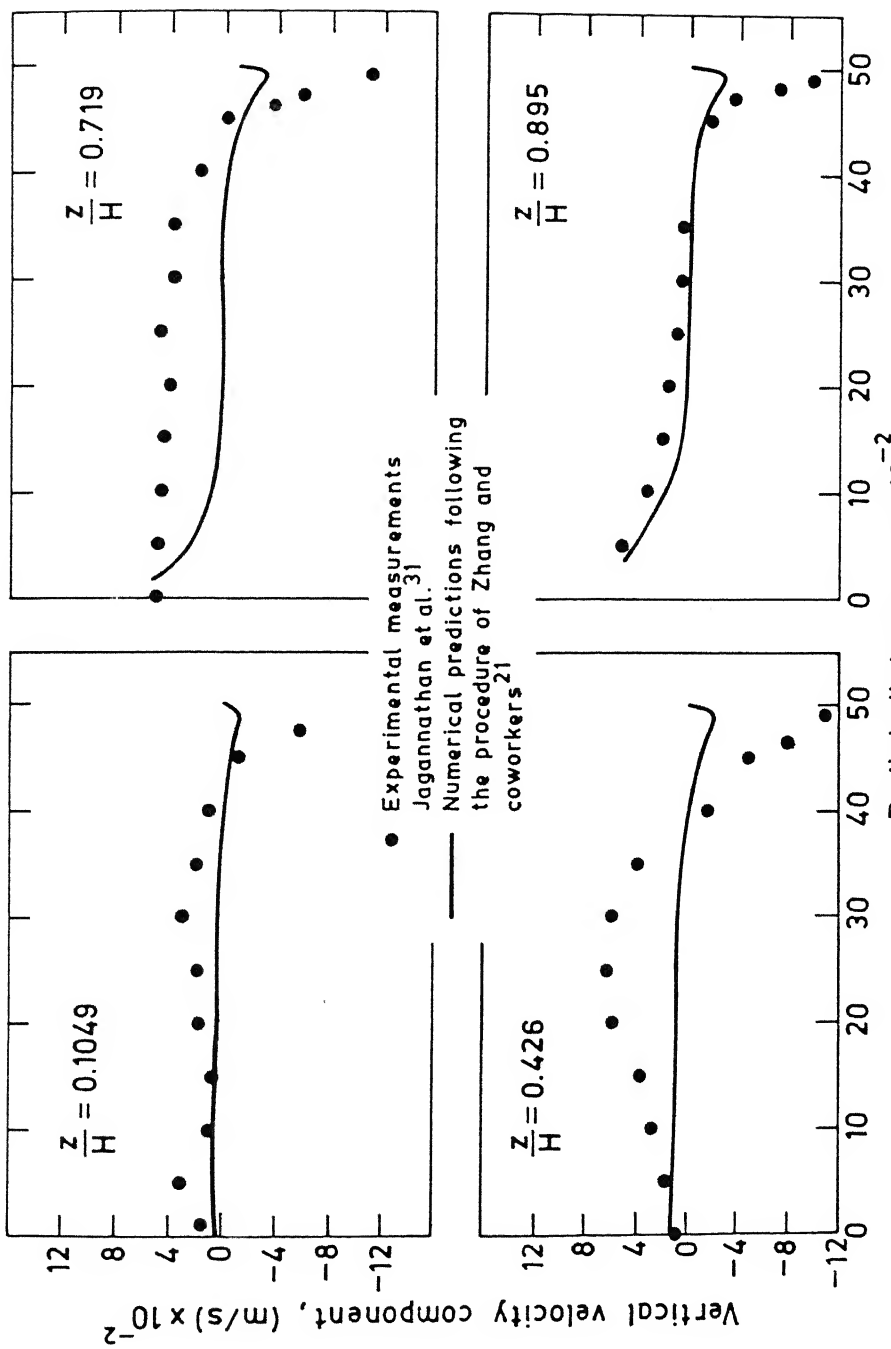

Fig. III.8. Numerically predicted vertical velocity component at different depths and their comparison with experimental measurements of Jagannathan et al.[31]

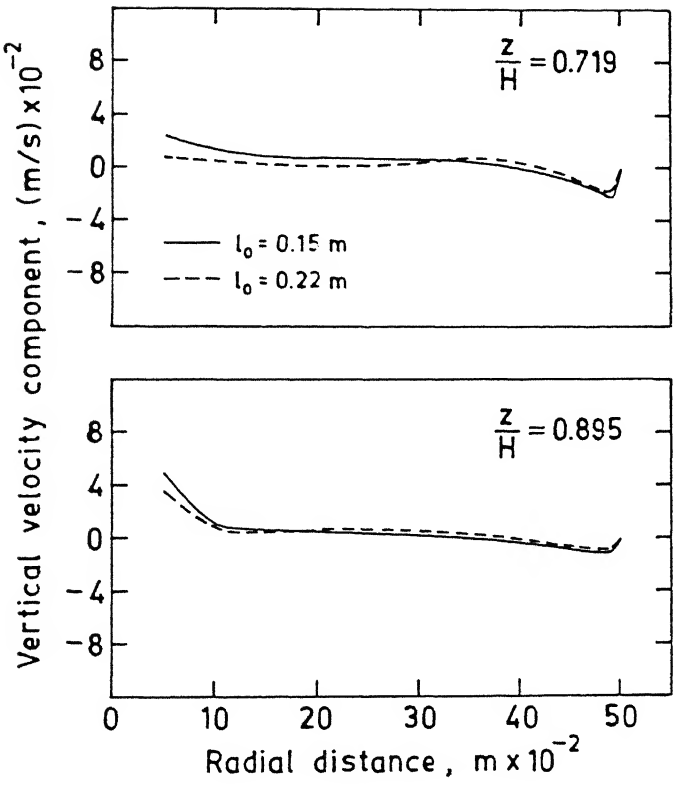

Fig. III.9. Sensitivity of numerical predictions to the values of l_o illustrating the variation of vertical velocity component at two different depths in the model reactor.

corresponding to Fig.III.8. The results have been illustrated in Fig.III.10 where the vertical velocity components at two different depths have been compared for two different set of values of the shear layer thickness. Clearly,the assumption of a shear layer thickness in the range Of 20-40 mm appears to be not critical to the overall prediction of the flow fields. These as a consequence suggest that uncertainities assosiated with the values of l_0 and the shear layer thickness are not likely to be the possible reasons for the discrepancy between theory and experiments illustrated in Fig.III.8.

III.3.2 Some additional considerations in the mathematical modelling of flows generated by an impinging gas jet

The impinging gas jet in a top blown system displaces fluid from the cavity region and consequently, leads to an infintismal increase in the bath height. Under steady state conditions when the bath height assumes a constant value during the injection process, it is readily apparent that some energy must be continuously fed into the system to sustain the increased bath height. Towards this, a sample calculation (corresponding to the experimental conditions of Jagannathan and coworkers[31]) suggests that displacement of fluid from the cavity region necessiates a force that is approximately equivalent about 13.8N while corresponding contribution from the integrated shear force appears to be only 6.213×10^{-2}N. Evidently, the shearing forces alone could not have produced the increased bath height and hence displace an equivalent amount of fluid from the cavity region. Consequently, it is legitimate to consider an appropriate gravity force (mass of the fluid displaced * accelaration due to gravity) in addition to the shearing forces, as an additional driving force

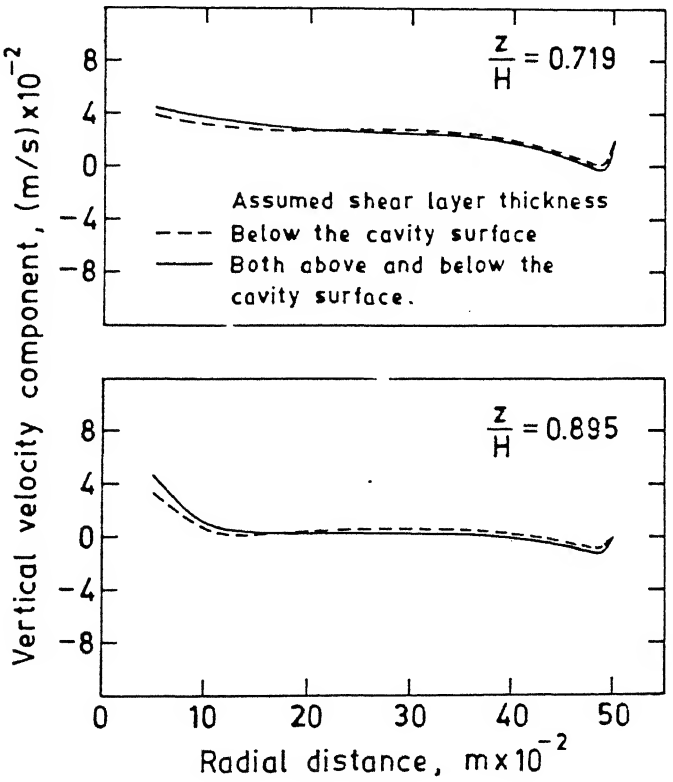

Fig. III.10. Sensitivity of numerical predictions to the choice of the shear layer thickness, illustrating the variation of vertical velocity component at two different depths in the model reactor.

producing the flow recirculation in such systems.

On the basis of these concepts, at each nodal point immediately below the cavity surface, a representative body force has been evaluated (viz.,interms of mass of displaced fluid and the acceleration due to gravity) added to the axial direction momentum equation in addition to the relevant shearing force components and the numerical predictions carried out again corresponding to the experimental conditions of Jagannathan and coworkers[31]. A comparison between predicted and experimental vertical velocity component at four different depths in the model has again been illustrated in Fig.III.11. The incorporation of the force of impingement into the mathematical model is clearly seen to produce estimates of flows that (in contrast to Fig.III.8) gives excellent agreement with the reported experimental measurements.

III.4 Mathematical Modelling Of The Combination Blown Process And comparison Of Numerical Predictions With Experimental Measurements

Mathematical modelling of the top as well as the bottom gas injection processes has been discussed extensively in the preceeding chapters. Since, the appropriate mechanisms of momentum transfer from gas to the liquid has been identified for both top and bottom gas injection systems, consequently, the concepts and the procedures can be combined to provide an effective hydrodynamic model for the analysis of the combination blown steelmaking process.

To assess the effectiveness of predictions via such an approach (viz.,coupling the models for bottom (section III.2.1.c) and top gas injection (section III.2.2)systems), calculations were performed corresponding to the experimewntal conditions of Zhang and coworkers[21]. These experimental conditions are summarised in Table

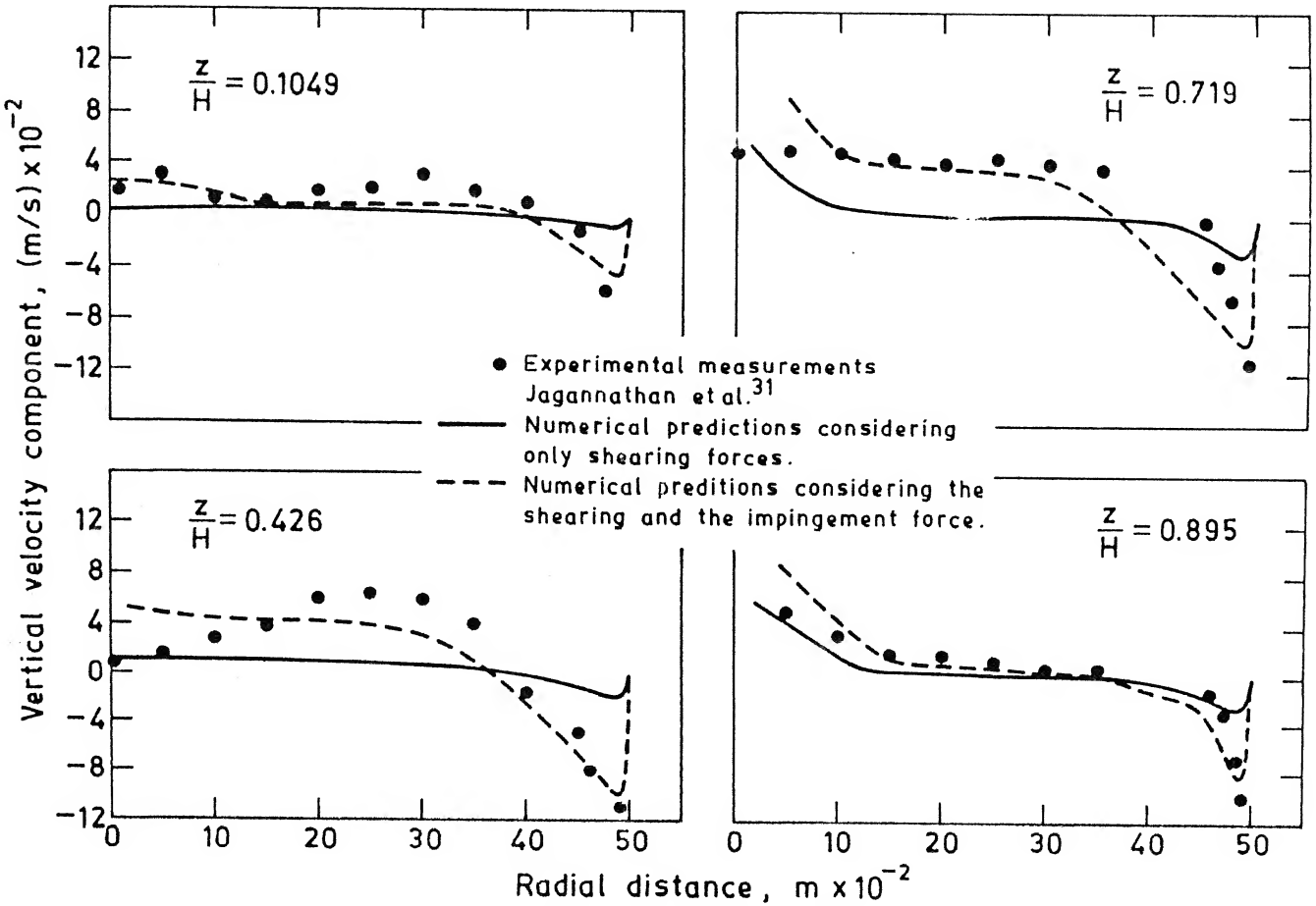

Fig. III.11. Numerically predicted vertical velocity component at different depths and their comparison with experimental measurements of Jagannathan et al.[31]

III.4. In Fig.III.12 numerically predicted flow patterns in the combination blown model vessel has been shown. This on comparison with equivalent experimental measurements of Zhang et al.[21] (see Fig.III.13) indicate reasonable agreement between theory and observations.

In deducing the results presented in Fig.III.12, the cavity volume has been artificially excluded from the domain of calculation by applying the 'cell porosity' concept of Moult and coworkers[26]. The principle involved has been briefly outlined in Fig.III.14. There, it is readily seen that by assigning a large S_p value to those nodal points within the cavity no flow condition can be at once prescribed. Similarly, for the control volumes lying partly within the cavity and partly within the bulk phase cell porosity factors (f's) have been estimated geometrically to deduce the effective convection and diffusion fluxes. Through this technique, the influence of the cavity surface and the cavity volume on the bulk phase hydrodynamics can be adequately taken into account.

Towards these, it is instructive to note here that numerical procedures of Zhang and coworkers[21] as well as that of Asai and Szekely[17] didnot consider the above and instead regarded the cavity as a part of the calculation domain. The cavity volume typically is much smaller (for the experimental conditions of Zhang et al.[21], cavity volume $\cong$ 0.1% of the reactor volume or cavity volume $\cong$ 5% of the plume volume) in comparison to that of the bulk and it may therefore appear at the first instance that inclusion/exclusion of the cavity volume into/from the calculation domain may not effect the predicted results significantly.

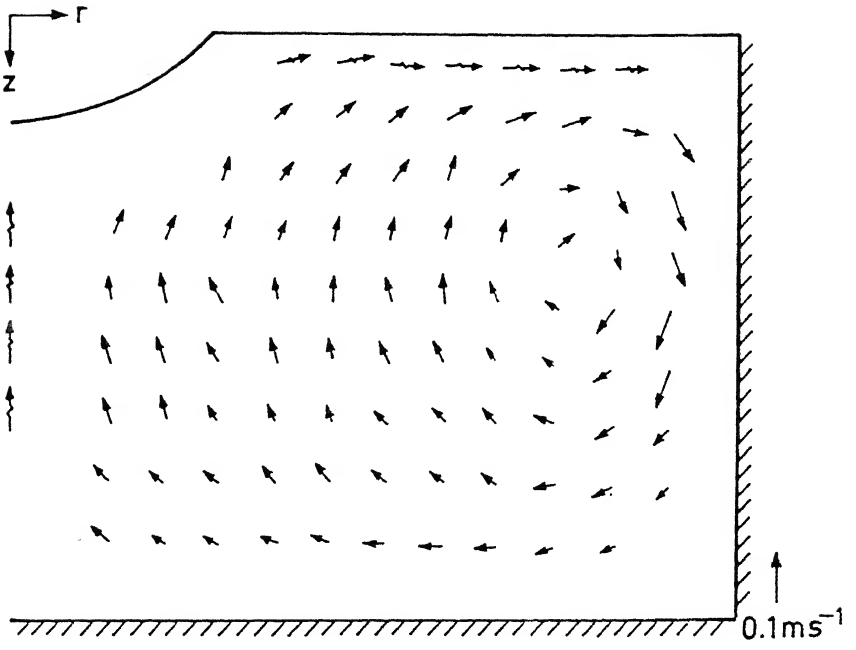

Fig III.12. Experimentally measured[21] velocity field in a water model of a combination blown steel making system.

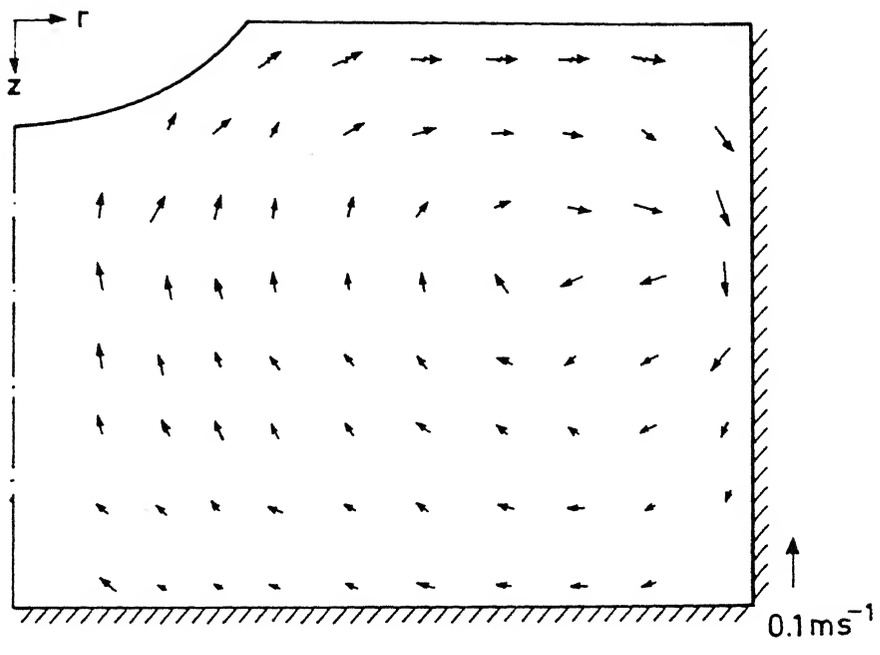

Fig. III.13. Numerically predicted flow field in a water model of a combination blown reactor (conditions corresponding to those of Zhang and coworkers[21]).

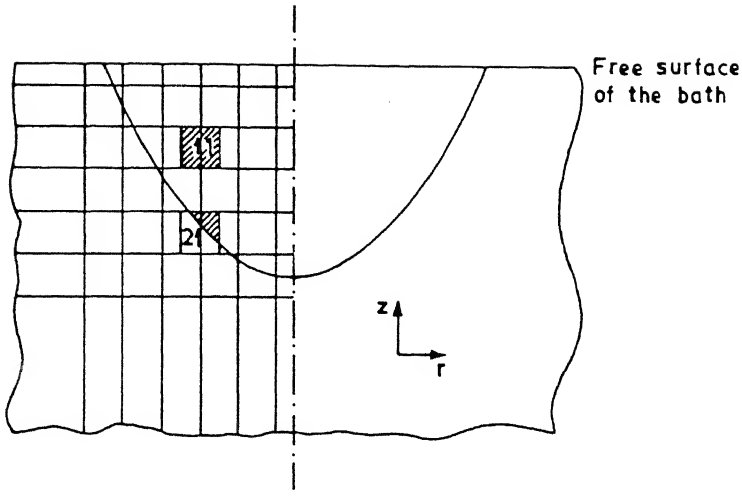

1. A completely blocked u control volume
   → $S_p = -10^{30}$ and $S_u = 0.0$
2. A partly blocked u control volume
   → $A_N = A_N$, $A_S = (1-f_1)A_S$, $A_E = (1-f_2)A_E$,
   $A_W = A_W$, f's are blockage ratios

Fig. III.14. The configuration of the cavity surface with reference to the finite difference grid, illustrating the principles involved in the cell porosity method applied to exclude the cavity volume from the domain of calculation.

Table III.4 Experimental conditions of different investigators used in the computation of results presented in Figs. III.7 through III.16.

	Experimental conditions of	
	Zhang and co-workers[21]	Jagannathan and co-workers[31]
Bath height, m	0.111	0.324
Radius of the vessel, m	0.145	0.5
Top gas flow rate, m^3/s	1.58×10^{-3}	8.33×10^{-3}
Bottom gas flow rate, m^{3}/s	3.75×10^{-5}	———
Inner diameter of orifice of lance nozzle, m	6×10^{-3}	2.3×10^{-3}
Distance between orifice of lance nozzle and free surface, m	0.154	0.15*
Depth of the bath cavity, m	0.0179	0.08
Radius of the bath cavity, m	0.0453	0.075

*Assumed

To test these, computations were carried out again for the experimental conditions of Zhang et al.[21] incorporating the cavity volume into the domain of calculation. In Fig.III.15 predicted vertical velocity component at two different depths in the model vessel have been compared with equivalent predictions ignoring the cavity volume. Clearly the predicted results, as one might have anticipated are not critical to either inclusion or exclusion of the cavity volume into/from the domain of calculation. It is important to note here that predicted vertical component of the flow deduced by ignoring the cavity, as seen from Fig.III.15 is somewhat larger than its counterpart. This to be expected since with the exclusion of the cavity from the calculation scheme, the net buoyancy force acting on the system is accordingly also under estimated and hence this leads to an overall slowering of fluid motion in the system. It is also reasonable to anticipate here that under such conditions if the gas volume fraction with in the plume is increased proportionately , the flows deduced from either of the calculation procedure would be practically equivalent.

Finally, in Fig.III.16, the corresponding assosiated turbulence kinetic energy field distribution is shown. This indicates that higher turbulent regions ($>10^{-2} m^2 s^{-2}$) are restricted close to the free surface region as well as the region immediately below the cavity while elsewhere, the turbulence kinetic energy is relatively low. Close to the bottom as well as the central portion of the reactor the turbulence is seen to be extremely low ($<10^{-4} m^2 s^{-2}$).These together with the predicted velocity fields may provide useful inferences about refractory wear, scrap melting etc. in an actual industrial steelmaking systems.

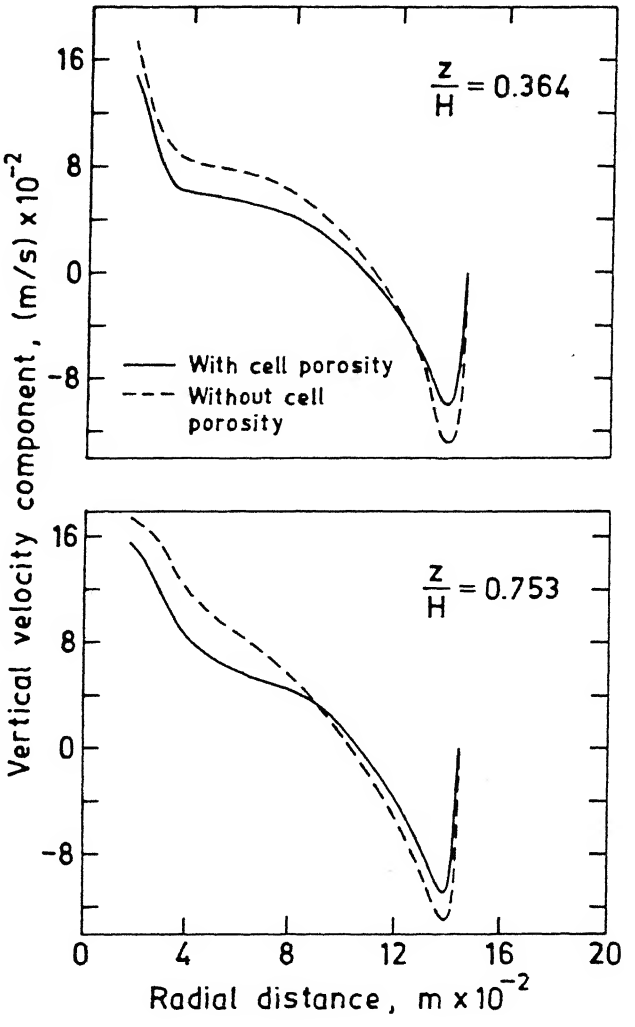

Fig. III.15. Theoretically predicted vertical velocity component at two different depths in the model vessel[21] illustrating the effect of considering/excluding the cavity volume on the computed results.

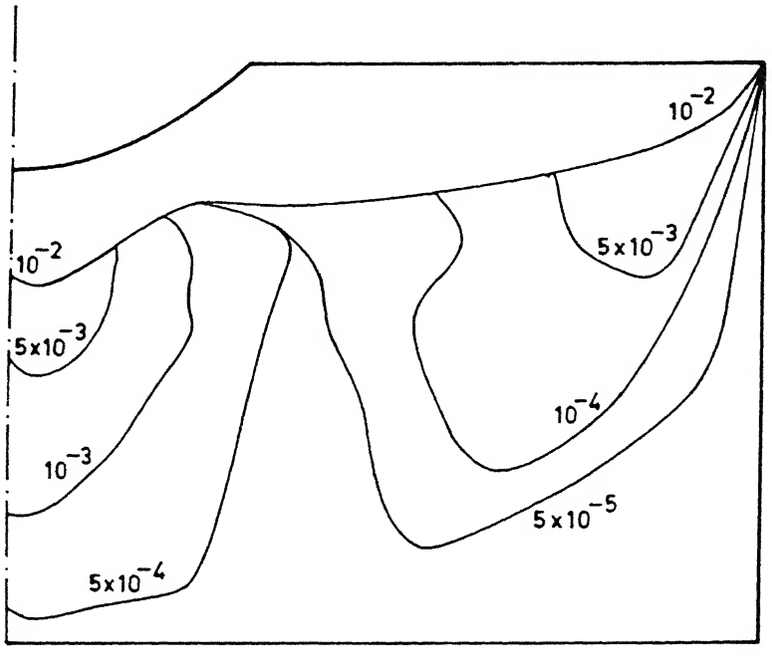

Fig. III.16. Prediction of turbulence kinetic energy (m^2s^{-2}) distribution in water model of a combination blown reactor (corresponding to the experimental conditions of Zhang et al.[21] as shown in Table III.4).

CHAPTER IV

CONCLUDING REMARKS

The following major conclusions can be drawn from the present investigation :

(1) Four different procedures to model the bottom gas injection phenomena (viz.,the bulk flow, the gas volume fraction in the plume etc.) have been rigorously assessed and it has been demonstrared that the buoyancy forces imparted by the rising bubbles in such systems is best represented if a constant plume rise velocity together with bubble slip is considered in the mathematical model.

(2) The comparisons between the theory and the experiments illustrate that the shearing forces imposed by the top gas injection are not likely to be the only mechanism producing the bath recirculation in top gas injection systems and that a mechanism such as the force of impingement (estimated interms of the appropriate gravity force) plays a crucial role in driving the flow field. This concept is new and is applied for the first time to model an impinging gas jet induced flow system.

(3) It has been shown that the force of impingement is many folds larger than the corresponding shear forces and consequently, an approach based on this has been adopted to model the top gas injection induced motion. The predicted results thus obtained are shown to agree reasonably well with the experimental observations reported in the literature.

(4) Numerically predicted results also indicate that estimates of velocity etc. in top or combination blown system are likeky to be relatively insensitive to the assumed shear layer thickness, provided a sufficiently large number of grid points are applied to the numerical solution scheme.

(5) In modelling the top gas injection induced flows, the cell porosity method has been applied to exclude the cavity volume from the calculation domain and the predicted results thus obtained indicate that exclusion/inclusion of cavity volume from/into the calculation domain have only marginal effect on the overall accuracy of predicted results.

(6) Combining the appropriate concepts for the top and the bottom gas injection procedures, a mathematical model for computation of flows in a combination blown steelmaking reactors has been developed and the numerical predictions evaluated against reported experimental measurements deduced from the water model studies and reasonable agreement between the two demonstrated.

CHAPTER V

RECOMMENDATIONS FOR FUTURE WORK

The scope of the present work can be further expanded considering the following :

(1) The axisymmetric mathematical model developed in the present study is to be applied to investigate mixing and mass-transfer phenomena in such systems.

(2) An idealised cylindrical vessel geometry has been considered in the development of the present model. The model must be made broad enough in its scope of computation so that an actual industrial configuration (which are slightly distorted cylinders) can be employed.

and finally,

(3) The axisymmetric model applied in the present study can be modified/improved to a fully three dimensional model so as to study theoretically the effect of multiple tuyeres or nozzle which are typical of industrial combination blown systems.

REFERENCES

1. M. P. Schwarz and W. J. Turner: Applied Mathematical Modelling., 1988, vol.12, pp. 273-279.
2. T. Debroy, A. K. Majumdar and D. B. Spalding: Applied Mathematical Modelling., 1978, vol.2, pp.146-150.
3. N. El-Kaddah and J. Szekely: Iron making and Steelmaking, 1981, vol.6, pp.269-278.
4. J. H. Grevet, J. Szekely and N. El-Kaddah: Int. J. of Heat and Mass Transfer, 1982, vol.25, pp.487-497.
5. Y. Sahai and R. I. L. Guthrie: Metall. Trans., 1982, vol.13B, pp.193-202.
6. Y. Sahai and R. I. L. Guthrie: Metall. Trans., 1982, vol.13B, pp.203-211.
7. D. Mazumdar and R. I. L. Guthrie: Metall. Trans., 1985, vol.16B, pp.83-90.
8. D. Mazumdar and R. I. L. Guthrie: Ironmaking and steelmaking., 1985, pp.725-733.
9. S. T. Johansen and F. Boysan: Metall. Trans., 1988, vol.19B, pp.755-764.
10. W. M. Pun and D. B. Spalding: Proceeding of the XVII International Astronautical Congress, 1967, vol.3, pp.3-21.
11. J. Szekely, H. J. Wang and K. M. Kiser: Metall. Trans., 1976, vol.7B, pp.287-295.
12. B. E. Launder and D. B. Spalding: Computer Methods in Applied Mechanics and Engineering., 1974, vol.3, pp.269-289.

13. T. C. Hsiao, T. Lehner and B. Kjellberg: Scand. J. Metallurgy., 1980, vol. 9, pp. 105-110.

14. M. Salcudean M. Low, C. H. Hurda and R. I. L. Guthrie: Chemical Engineering communication., 1983, vol. 21, pp. 89-96.

15. L. W. Frech: Ironmaking and Steelmaking., 1979, no. 3, pp. 110-113.

16. M. Saigusa, F. Sudo and S. Yamada: Ironmaking and Steelmaking., 1980, pp. 242-248.

17. J. Szekely and S. Asai: Metall. Trans., 1974, vol. 5, pp. 463-467.

18. A. D. Gosman, W. M. Pun, A. K. Runchal, D. B. Spalding and M. Wolshtein: Heat andMass Transfer In Recirculating Flows., Academic Press, London, 1969, pp. 18-112.

19. A. N. Kolmogorov and L. Prandtl: Izv. Akad Naut SSSR. Ser. Phys., 1952, vol. 7, pp. 56.

20. D. H. Wakelin: Ph. D Thesis., University of London, England, 1966.

21. J. Zhang, S. Du and S. Wei: Ironmaking and Steelmaking., 1985, vol. 12, pp. 249-255.

22. J. szekely: Fluid Flow Phenomenon In Metal Processing., Academic Press, 1971.

23. S. V. Patankar: Numerical Heat Transfer and Fluid FLow., Hemisphere Publishing corporation, New York, 1980.

24. S. V. Patankar and D. B. Spalding: Int. Journal of Heat and Mass Transfer., 1972, vol. 15, pp. 1787-1805.

25. D. B. Spalding: Heat Transfer and Turbulent Buoyant Convection., Hemisphere Publishing Corporation, New York, 1977, pp. 569-586.

26. A. Moult, D. B. Spalding and N. C. Markatos: Transaction of Institution of Chemical Engineers, 1979, vol. 57, pp. 200-204.

27. D. Mazumdar H. Nakajima and R. I. L. Guthrie: Metall. Trans., 1988, vol. 19B, pp. 507-511.

28. D. Mazumdar and R. I. L. Guthrie: Ironmaking and Steelmaking (in press).

29. B. Carnhan, H. A. Luther and J. O. Wilkes: Applied Numerical Methods., John Wiley and sons, New York, 1969.

30. A. H. Castillejos and J. K. Brimacombe: Metall. Trans., 1987, vol. 18B, pp. 659-671.

31. K. P. Jagannathan, T. K. Parihar and S. R. Ghantasala: Intl. Conf on "Progress in Metallurgical Research: Fundamental and applied Aspects", T. R. Ramachandran and S. P. Mehrotra 1985, IIT Kanpur, India.

APPENDIX

```
C           TO FIND THE SOLUTION OF A DIFFERENTIAL EQUATION
C           du(z)/dz + u(z)/z = pi*Q*g/(2(tan(lamada)*u(z)*z)**2) BY
C           RUNGA-KUTTA METHOD WITH THE HELP OF GIVEN BOUNDARY
C           CONDITIONS z=z(1),u(z)=u(0). THE SOLUTION OF THE ABOVE
C           DIFFERENTIAL EQUATION GIVES THE VELOCITY AS A FUNCTION
C           OF z.

            OPEN(UNIT=23,FILE='RUNGA.IN')
            OPEN(UNIT=22,FILE='RUNGA.OUT')
            IMPLICIT REAL*8(A-H,O-Z)
            DIMENSION Z(50),U(50),ALFA(50),R(50)
            READ(23,*)  (R(N),N=1,21)
            Z(1)=0.01842
            U(1)=18.86
            US=0.2259
            H=0.003335
            NMAX=21
            PI=3.14
            Q=3.3333E-05
            G=9.81
            TANLAM=0.086
            DO 20 N=1,NMAX-1
            S1=PI*Q*G/(2*(TANLAM*U(N)*Z(N))**2)-U(N)/Z(N)
            Z(N)=Z(N)+H/2
            U(N)=U(N)+S1*(H/2)
            S2=PI*Q*G/(2*(TANLAM*U(N)*Z(N))**2)-U(N)/Z(N)
            Z(N)=Z(N)+H/2
            U(N)=U(N)+S2*(H/2)
            S3=PI*Q*G/(2(TANLAM*U(N)*Z(N))**2)-U(N)/Z(N)
            Z(N)=Z(N)+H
            U(N)=U(N)+S3*H
            S4=PI*Q*G/(2(TANLAM*U(N)*Z(N)))**2)-U(N)/Z(N)
            Z(N+1)=Z(N)+H
            U(N+1)=U(N)+(H/6)*(S1+2*S2+2*S3+S4)
20          CONTINUE
            DO 40 N=1,NMAX
            A=PI*R(N)**2*(U(N+1)+US)
            F=4.0*PI*R(N)**2*US*Q
            P=2.0*PI*R(N)**2*US
            ALFA(N)=A/P-(DSQRT(A**2-F))/P
40          CONTINUE
            WRITE(22,400)
400         FORMAT(8X,'NO',9X,'Z(M)',9X,'VEL(m/s)',8X,'RAD(M)'
        1   ,'6X,'ALFA(N)'/)
            DO 30 N=1,NMAX
            WRITE(22,500) N,Z(N),U(N),R(N),ALFA(N)
500         FORMAT(5X,I4,5X,F10.4,5X,F10.4,5X,F10.4,3X,F10.6/)
30          CONTINUE
            STOP
            END
```